

© 2019 by Gwendolyn J. Chee. All rights reserved.

SENSITIVITY ANALYSIS OF NUCLEAR FUEL CYCLE TRANSITIONS

BY

GWENDOLYN J. CHEE

THESIS

Submitted in partial fulfillment of the requirements  
for the degree of Master of Science in Nuclear, Plasma, and Radiological Engineering  
in the Graduate College of the  
University of Illinois at Urbana-Champaign, 2019

Urbana, Illinois

Master's Committee:

Assistant Professor Kathryn D. Huff, Advisor  
Professor James F. Stubbins

# Abstract

The present United States nuclear fuel cycle faces challenges that hinder the expansion of nuclear energy technology. The U.S. Department of Energy identified four classes of nuclear fuel cycle options the U.S could transition to, which would overcome these challenges and make nuclear energy technology more desirable. The transitions have been modeled by various nuclear fuel cycle simulators. However, most fuel cycle simulators require the user to define a deployment scheme for all supporting facilities to avoid any supply chain gaps, which becomes tedious for complex transition scenarios. This thesis developed a capability in CYCLUS, a nuclear fuel cycle simulator, to automatically deploy fuel cycle facilities to meet user-defined power demand. This new capability successfully deployed fuel cycle facilities in a transition scenario from the current light water reactor fleet to a closed fuel cycle with continuous recycling of transuramics in fast and thermal reactors. In reality, these transition scenarios inevitably diverge from the modeled scenario. This work coupled the nuclear fuel cycle simulator tools, CYCLUS and DYMOND, with Dakota, a sensitivity analysis toolkit. This work conducted one-at-a-time, synergistic, and global sensitivity analysis with CYCLUS-Dakota and DYMOND-Dakota, to understand the interdependence of input parameters on the transition performance from the current light water reactor fleet to a closed fuel cycle in which transuramics are recycled to fuel mixed oxide fuel thermal reactors and sodium fast-cooled reactors. The global sensitivity analysis concluded that the transition year input parameter was the most influential to the final depleted uranium and total idle reactor capacity performance metrics, and the fleet share ratio and cooling time input parameters were the most influential to the final high level waste amount in the simulation. The one-at-a-time sensitivity analysis showed that varying transition year from 80 to 84 years increased the final depleted uranium amount by 1.13% and reduced the total idle reactor capacity by 10.36%. The one-at-a-time sensitivity analysis also showed that varying fleet share ratio (mixed oxide fuel light water reactor: sodium fast-cooled

reactor) from 0:100 to 20:80 reduced the final high level waste amount by 2%, and varying the used fuel cooling time from 0 to 8 years reduced the final high level waste amount by 4%. Therefore, an optimized transition scenario that minimizes final high level waste amount, final depleted uranium amount, and total idle capacity must have a fleet share ratio of 20:80, used fuel cooling time of 8 years, and a transition year at 83 years. This work compared CYCLUS-Dakota's and DYMOND-Dakota's sensitivity analysis capabilities and concluded that automated deployment of supporting fuel cycle facilities is crucial for conducting sensitivity analyses with nuclear fuel cycle simulators, to ensure that the simulation adapts to the new parameters by minimizing idle reactor capacity. The results demonstrated that time is saved if a comprehensive sensitivity analysis of a nuclear fuel cycle transition scenario begins with a global sensitivity analysis study to gain a general overview of the influential input variables for the performance metrics. Then, based on the global sensitivity analysis results, a reduced number of one-at-a-time and synergistic sensitivity analyses are conducted to determine quantitative trends and impacts of influential input variables on the performance metrics.

*To my mother, I couldn't have done it without you!*

# Acknowledgments

I want to express my deepest gratitude to my advisor, Dr. Kathryn Huff, for her guidance, patience, and support in my learning journey towards becoming a proper scientist. I also wish to thank Dr. Bo Feng from Argonne National Laboratory for his guidance in conducting sensitivity analysis studies and invaluable career advice. I would also like to acknowledge Dr. James Stubbins as the second reader of this thesis; I am grateful for his valuable comments on this thesis. This work would not have been possible without the financial support of the Nuclear Energy University Program for funding me through the ‘Demand-Driven Cycamore Archetypes’ project (Project 16-10512, DE-NE0008567).

I thank my fellow groupmates, for the embodiment of ‘misery loves company’, Greg Westphal, Jin Whan Bae, Sun Myung Park, Roberto Fairhurst, Anshuman Chaube, Kip Kleimenhagen, Gyu Tae Park, Andrei Rykhlevskii, and Sam Dotson. Special thanks to Kip Kleimenhagen for his excellent proofreading. I also had the pleasure of collaborating with the wonderful and supportive Cyclus community, particularly those in the University of Wisconsin Computational Nuclear Engineering Research Group (CNERG) and the University of South Carolina Energy Research Group (ERGS). I am also grateful to my WiN family for my weekly dose of good vibes and rapport. Special thanks to my roommate, Mao, who always brightened my day with baked goods and funny memes.

Finally, I cannot begin to express my thanks to my parents, Joy and Gerard, and my brother, Ben, for their unwavering love and support from day one.

# Table of Contents

<b>List of Tables . . . . .</b>	<b>viii</b>
<b>List of Figures . . . . .</b>	<b>xi</b>
<b>Chapter 1 Introduction . . . . .</b>	<b>1</b>
1.1 Motivation . . . . .	1
1.2 Objectives . . . . .	3
<b>Chapter 2 Literature Review . . . . .</b>	<b>4</b>
2.1 Nuclear Fuel Cycle Simulator History . . . . .	4
2.2 Transition Scenario Capabilities in Nuclear Fuel Cycle Simulators . . . . .	6
2.3 Sensitivity Analysis Studies . . . . .	7
2.3.1 One-at-a-time Sensitivity Analysis . . . . .	8
2.3.2 Synergistic Sensitivity Analysis . . . . .	8
2.3.3 Global Sensitivity Analysis . . . . .	10
2.3.4 Summary of Sensitivity Analysis Studies . . . . .	13
<b>Chapter 3 Methods . . . . .</b>	<b>14</b>
3.1 CYCLUS . . . . .	14
3.2 Demand driven deployment capability in CYCLUS ( <i>d3ploy</i> ) . . . . .	15
3.2.1 <i>d3ploy</i> framework . . . . .	16
3.3 DYMOND . . . . .	29
3.4 Sensitivity Analysis Capabilities . . . . .	30
3.4.1 DYMOND-Dakota Coupling ( <i>ddwrapper</i> ) . . . . .	30
3.4.2 CYCLUS-Dakota Coupling ( <i>dcwrapper</i> ) . . . . .	31
3.5 Chapter Summary . . . . .	31
<b>Chapter 4 Results: <i>d3ploy</i> Demonstration . . . . .</b>	<b>32</b>
4.1 <i>d3ploy</i> Demonstration of Simple Transition Scenarios . . . . .	32
4.1.1 Simple Transition Scenario Simulation: Constant Demand . . . . .	32
4.1.2 Simple Transition Scenario Simulation: Linearly Increasing Demand . . . . .	34
4.1.3 Simple Transition Scenario Simulation: Sinusoidal Demand . . . . .	36
4.2 <i>d3ploy</i> Demonstration of EG01-30 Transition Scenario . . . . .	36
4.2.1 Comparison of Prediction Methods . . . . .	40
4.2.2 Comparison of Power Buffer Sizes . . . . .	43
4.2.3 Demonstration of Best Performance Model . . . . .	45
4.3 Chapter Summary . . . . .	45

<b>Chapter 5 Results: Sensitivity Analysis</b>	<b>48</b>
5.1 Transition Scenario Specification	48
5.1.1 DYMOND	49
5.1.2 CYCLUS	49
5.2 Sensitivity Analysis: Evaluation Metrics	50
5.3 One-at-a-time Sensitivity Analysis	52
5.3.1 Length of cooling time for used fuel	52
5.3.2 Fleet share ratio of PWR MOX and SFR reactors	55
5.3.3 Introduction year of advanced reactor technology	57
5.4 Synergistic Sensitivity Analysis	61
5.4.1 Fleet Share Ratio and Introduction date of advanced reactor technology	61
5.5 Global Sensitivity Analysis	64
5.6 Chapter Summary	67
5.6.1 DYMOND Limitations	67
5.6.2 Importance of Different Types of Sensitivity Analysis	67
<b>Chapter 6 Conclusion</b>	<b>68</b>
6.1 Contributions	68
6.2 Suggested Future Work	69
<b>References</b>	<b>71</b>

# List of Tables

2.1	Nuclear fuel cycle simulator tools and their corresponding organizations. . . . .	5
3.1	d3ploy's required and optional input parameters with examples. . . . .	21
4.1	d3ploy's input parameters for the simple constant, linearly increasing, and sinusoidal power demand transition scenarios. . . . .	33
4.2	The total number of time steps with commodity undersupply for each simple transition scenario. . . . .	38
4.3	Total number of time steps with power undersupply for the EG01-30 transition scenario for different prediction methods. . . . .	43
4.4	Dependency of the power undersupply on the buffer size for EG01-EG30 transition scenarios with linearly increasing power demand using the FFT prediction method. There is less power undersupply for a larger power buffer size. . . . .	45
4.5	d3ploy's input parameters for the EG01-EG30 transition scenario which minimize undersupply for power and minimizes the undersupply and under capacity for other facilities. . . . .	47
5.1	OECD Benchmark Transition Scenario Specifications [34] . . . . .	49
5.2	CYCLUS facility input parameters for EG01-EG30 transition scenario that minimizes undersupply of power and minimizes the undersupply and under capacity of other commodities. . . . .	50
5.3	Evaluation metrics and their associated output variables. . . . .	52
5.4	DYMOND: Assessment of the impact of used fuel cooling time variation on evaluation metrics (waste management, resource utilization, and goodness of transition) for the OECD benchmark transition scenario [7]. . . . .	53
5.5	DYMOND: Assessment of the impact of used fuel cooling time variation on evaluation metrics (proliferation risk) for the OECD benchmark transition scenario [7]. . . . .	54
5.6	DYMOND: Impact of variation in used fuel cooling times on evaluation metrics (waste management, resource utilization, and goodness of transition) for OECD benchmark transition scenario. The numbers in the table represent the percentage difference between an output variable from each scenario and the base case scenario (Cooling time = 2 years) [7]. . . . .	54
5.7	DYMOND: Impact of variation in used fuel cooling times on evaluation metrics (proliferation risk) for OECD benchmark transition scenario. The numbers in the table represent the percentage difference between an output variable from each scenario and the base case scenario (Cooling time = 2 years) [7]. . . . .	55

5.8 CYCLUS: Assessment of the impact of used fuel cooling time variation on evaluation metrics (waste management, resource utilization, and goodness of transition) for EG01-EG30 transition scenario [10]. . . . .	56
5.9 CYCLUS: Assessment of the impact of used fuel cooling time variation on evaluation metrics (proliferation risk) for EG01-EG30 transition scenario [10]. . . . .	56
5.10 CYCLUS: Impact of variation in used fuel cooling times on evaluation metrics (environmental impact, resource utilization, and goodness of transition) for EG01-EG30 transition scenario. The numbers in the table represent the percentage difference between an output variable from each scenario and the base case scenario (Cooling time = 2 years) [10]. . . . .	56
5.11 CYCLUS: Impact of variation in used fuel cooling times on evaluation metrics (proliferation risk) for EG01-EG30 transition scenario. The numbers in the table represent the percentage difference between an output variable from each scenario and the base case scenario (Cooling time = 2 years) [10]. . . . .	57
5.12 CYCLUS: Assessment of the impact of variation in fleet share ratio of LWR MOX and SFR reactors on evaluation metrics (environmental impact, resource utilization, and goodness of transition) for EG01-30 transition scenario [10]. . . . .	58
5.13 CYCLUS: Assessment of the impact of variation in fleet share ratio of LWR MOX and SFR reactors on evaluation metrics (proliferation risk) for EG01-30 transition scenario [10]. . . . .	58
5.14 CYCLUS: Impact of variation in fleet share ratio of LWR MOX and SFR reactors on evaluation metrics (environmental impact, resource utilization, and goodness of transition) for EG01-EG30 transition scenario. The numbers in the table represent the percentage difference between an output variable from each scenario and the base case scenario (PWR MOX fleet share = 15%) [10]. . . . .	58
5.15 CYCLUS: Impact of variation in fleet share ratio of LWR MOX and SFR reactors on evaluation metrics (proliferation risk) for EG01-EG30 transition scenario. The numbers in the table represent the percentage difference between an output variable from each scenario and the base case scenario (PWR MOX fleet share = 15%) [10]. . . . .	59
5.16 CYCLUS: Assessment of impact of variation in advanced reactor introduction year on evaluation metrics (environmental impact, resource utilization, and goodness of transition) for EG01-30 transition scenario [10]. . . . .	60
5.17 CYCLUS: Assessment of impact of variation in advanced reactor introduction year on evaluation metrics (proliferation risk) for EG01-30 transition scenario [10]. . . . .	60
5.18 CYCLUS: Impact of variation in advanced reactor introduction year on evaluation metrics (environmental impact, resource utilization, and goodness of transition) for EG01-EG30 transition scenario. The numbers in the table represent the percentage difference between an output variable from each scenario and the base case scenario (transition year = 80) [10]. . . . .	60
5.19 CYCLUS: Impact of variation in advanced reactor introduction year on evaluation metrics (proliferation risk) for EG01-EG30 transition scenario. The numbers in the table represent the percentage difference between an output variable from each scenario and the base case scenario (transition year = 80) [10]. . . . .	61



# List of Figures

2.1	Overall results from OECD one-at-a-time sensitivity analysis study. This is reproduced from the OECD report [1]. Sensitivity Table with an overview of all the sensitivity indicators S obtained from the various input parameters (one row for each input parameter) and the various output parameters (one column for each output parameter). When a sensitivity coefficient is positive (red), this means an increase of the input parameter induces an increase of the output parameter. Whereas, when it is blue, this means an increase of the input parameter induces a decrease of the output parameter. When a coefficient of determination $r^2$ is lower than 0.9, then the related sensitivity indicator is replaced by a question mark ? in the table. When the output parameter is not impacted by the variation of the input parameter, then the related sensitivity indicator is not available and it is replaced by a blank in the table. [1]. . . . .	9
2.2	A tornado plot from the OECD one-at-a-time sensitivity analysis study, showing the sensitivity of the separated Pu in storage amount to each input parameter. This is reproduced from the OECD report [1]. . . . .	10
2.3	Payoff surface for variation in thermal reprocessing and fast reactor technology introduction date [36]. The payoff surface represents a combination of weighted optimization criteria: minimize construction of reprocessing plants, minimize leveled cost of electricity (LCOE), minimize depleted uranium generated, and minimize total SWU used. . . . .	11
3.1	The CYCLUS core provides an application programming interface (API) to modularly load user-selected archetypes into the CYCLUS simulation [23]. . . . .	15
3.2	d3ploy logic flow at every timestep in CYCLUS [8]. . . . .	17
3.3	Simple once-through fuel cycle depicting which facilities are deployed by DemandDrivenDeploymentInst and SupplyDrivenDeploymentInst. . . . .	19
3.4	d3ploy has a $100 - t$ preference for LWRs and a $t - 99$ preference for SFRs. When there is a power undersupply, d3ploy will deploy the reactor that has a larger preference at that time step. . . . .	23
3.5	Logical flow of how d3ploy selects which facility to deploy when there are multiple facilities offering the same commodity. . . . .	24
3.6	Depiction of the coupling of Dakota and each nuclear fuel cycle (NFC) code. . . . .	30
4.1	Power demand curves for the simple constant, linearly increasing, and sinusoidal power demand transition scenarios. . . . .	33

4.2	Power demand and supply, and reactor facility deployment for a simple constant power demand transition scenario with three facility types: <code>source</code> , <code>reactor</code> , and <code>sink</code> . There are no time steps with power undersupply [9] . . . . .	34
4.3	Simple constant power demand transition scenario with three facility types: <code>source</code> , <code>reactor</code> , and <code>sink</code> . . . . .	35
4.4	Power demand and supply, and reactor facility deployment plot for a simple linearly increasing power demand transition scenario with three facility types: <code>source</code> , <code>reactor</code> , and <code>sink</code> . There are no time steps with power undersupply[9]. . . . .	36
4.5	Simple linearly increasing power demand transition scenario with three facility types: <code>source</code> , <code>reactor</code> , and <code>sink</code> . . . . .	37
4.6	Power demand and supply, and reactor facility deployment plot for a simple sinusoidal power demand transition scenario with three facility types: <code>source</code> , <code>reactor</code> , and <code>sink</code> . There are no time steps with power undersupply [9]. . . . .	38
4.7	Simple sinusoidal power demand transition scenario with three facility types: <code>source</code> , <code>reactor</code> , and <code>sink</code> . . . . .	39
4.8	Facility and mass flow for the EG01-EG30 transition scenario. EG01 is the current once through LWR fuel cycle. EG30 is a closed fuel cycle with continuous recycling of U/TRU in fast and thermal reactors. . . . .	41
4.9	EG01-30 transition scenario with linearly increasing power demand. Each subplot shows the total number of time steps in which there exists undersupply and under capacity of commodities for each prediction method. The different colors represent different commodities, and each vertical bar refers to 50 time steps in the simulation. The FFT and POLY prediction methods perform the best, with the fewest time steps with undersupply and undercapacity [9]. . . . .	42
4.10	The effect of power buffer size on power undersupply for the EG01-30 transition scenario with linearly increasing power demand using the FFT method. . . . .	44
4.11	Time dependent deployment of reactor and supporting facilities in the EG01-30 linearly increasing power demand transition scenario. <code>d3ploy</code> automatically deploys reactor and supporting facilities to setup a supply chain to meet linearly increasing power demand of $60000+250t/12$ MW during a transition from Light Water Reactors (LWRs) to MOX LWRs and Sodium-Cooled Fast Reactors (SFRs) [9]. . . . .	46
5.1	DYMOND EG01-30 Transition Scenario: Maximum amount of Pu [kg] in each inventory for varying fleet share and transition start date simulations [7]. . . . .	63
5.2	Impact on final amount of HLW [kg] when fleet share and transition start date are varied for the CYCLUS EG01-30 transition scenario [10]. . . . .	64
5.3	Impact on final amount of Depleted Uranium [kg] when fleet share and transition start date are varied for the CYCLUS EG01-30 transition scenario [10]. . . . .	65
5.4	Impact on total amount of idle reactor capacity [MW] when fleet share and transition start date are varied for the CYCLUS EG01-30 transition scenario [10]. . . . .	65

# Chapter 1

## Introduction

### 1.1 Motivation

The impact of climate change on natural and human systems is increasingly apparent [2]. Increases in global average surface temperatures, sea levels, and larger climate extremes are a few consequences brought on by elevated Greenhouse Gas (GHG) concentrations [2]. Energy use and production contribute to two-thirds of the total GHG emissions [2]. Furthermore, as the human population increases and previously under-developed nations rapidly urbanize, global energy demand is forecasted to increase. Energy generation technology selection profoundly impacts climate change via growing energy demand. Large scale deployment of emissions free nuclear power plants could significantly reduce GHG production [2].

However, large scale nuclear power deployment faces challenges of cost, safety, and used nuclear fuel [38]. Nuclear power has high capital costs, an unresolved long-term nuclear waste management strategy and perceived adverse safety, environmental, and health effects [38]. The nuclear power industry must overcome these challenges to ensure continued global use and expansion of nuclear energy technology.

The challenges described above are associated with the present once-through fuel cycle in the United States (US), in which fabricated nuclear fuel is used once and placed into storage to await disposal. To overcome these challenges, nuclear fuel cycle simulator tools are used to explore long-term behavior and performance of alternative fuel cycles. Nuclear fuel cycle simulators are used to evaluate the impact of nuclear fuel cycles at both high and low resolution. These simulators track the flow of materials through the nuclear fuel cycle, from enrichment to final disposal of the fuel, while also accounting for decay and transmutation of isotopes. The impacts are evaluated in the form of ‘metrics’, quantitative measures of performance [23]. These metrics are calculated

from mass balances and facility operation histories calculated by a fuel cycle simulator [23]. By evaluating performance metrics of different fuel cycles, we gain an understanding of how each facility’s parameters and technology choices impact the system’s performance. Therefore, these results are used by DOE to inform research direction and funding decisions, and advise future reactor design choices [52].

The Office of Nuclear Energy’s Fuel Cycle Options (FCO) Campaign led an evaluation and screening study of a comprehensive set of nuclear FCOs to identify FCOs with the potential to substantially improve the nuclear fuel cycle in the challenge areas [51]. The study concluded that fuel cycles with continuous recycling of co-extracted U/Pu or U/TRU in fast spectrum critical reactors consistently scored high overall performance in the following categories: used nuclear fuel management, environmental impact, and resource utilization. The evaluation and screening study assumed the nuclear energy systems were at equilibrium to understand each Evaluation Group’s end-state benefits [14]. Therefore, evaluation of the dynamics of transitioning from the current once-through fuel cycle to these promising future end-states [14] is the logical next step, propelling this nuclear fuel cycle transition scenario analysis research.

Nuclear fuel cycle simulation tools must automate the transition scenario simulation setup to successfully model a time-dependent transition scenario. Many existing nuclear fuel cycle simulator tools have conducted transition scenario analyses [14, 4, 11] and faced challenges stemming from the vast input parameter sample space. Since many of these input parameters are coupled, it is a tedious process to use trial and error to manually find a balance between various input parameters to set up a successful transition scenario. We define a successful transition scenario simulation as one that has a minimal power undersupply, minimal undersupply, and oversupply of all commodities.

In reality, the real transition process inevitably diverges from the modeled transition scenario. It is insufficient to set up only one transition scenario to model nuclear power’s future projections. Therefore, it is imperative to conduct sensitivity analysis to understand the effect of variation in input parameters on performance metrics.

## 1.2 Objectives

This thesis' objectives were developed based on the difficulties nuclear fuel cycle simulators face when modeling transition scenarios and conducting sensitivity analysis in the context of those scenarios. Accordingly, the objectives are listed below.

**Develop a capability in Cyclus [23], a nuclear fuel cycle simulator, to ease the setup of transition scenarios.** Due to the interdependence of many nuclear fuel cycle input parameters, nuclear fuel cycle simulator users' must manually determine each facility's deployment schedule to avoid supply chain gaps. Thus, a next-generation nuclear fuel cycle simulator must automate transition scenario setup by predictively and automatically deploying fuel cycle facilities to meet user-defined power demand.

**Develop sensitivity analysis capabilities in the Cyclus and DYMOND nuclear fuel cycle simulators.** Sensitivity analysis identifies areas in the nuclear fuel cycle that highly influence performance metrics. We leverage Dakota [12], a well supported sensitivity analysis tool, to introduce sensitivity analysis capabilities to CYCLUS and DYMOND.

**Demonstrate Cyclus transition scenario setup using the developed capability.** We demonstrate successful implementation of CYCLUS' automated transition scenario setup capability by setting up a simple three-facility transition scenario and a complex closed fuel cycle transition scenario.

**Use Cyclus and DYMOND to conduct sensitivity studies.** We demonstrate one-at-a-time, synergistic, and global sensitivity analysis with CYCLUS-Dakota and DYMOND-Dakota.

**Compare Cyclus-Dakota's and DYMOND-Dakota's capabilities in conducting sensitivity analysis.** DYMOND lacks the automated transition scenario setup capability that was developed for CYCLUS. Through comparison of sensitivity analysis studies conducted by CYCLUS-Dakota and DYMOND-Dakota, we demonstrate the importance of automated transition scenario setup capability in nuclear fuel cycle simulators.

# Chapter 2

## Literature Review

### 2.1 Nuclear Fuel Cycle Simulator History

The nuclear fuel cycle represents the nuclear fuel life cycle from initial extraction through processing, use in reactors, and, eventually, final disposal. This complex system of facilities and mass flows collectively provide nuclear energy in the form of electricity [52]. A closed nuclear fuel cycle reprocesses used fuel, whereas an open nuclear fuel cycle does not. The US has an open nuclear fuel cycle; other countries, such as France, have a closed nuclear fuel cycle.

Nuclear fuel cycle system analysis tools were introduced to investigate nuclear fuel cycle dynamics at a local and global level. Nuclear fuel cycle simulators' primary purpose is to understand the dependence between various system designs, deployment strategies, and technology choices in the nuclear fuel cycle and the impact their variations have on the system's performance. Nuclear fuel cycle simulator results are used to guide research efforts, advise future design choices, and provide decision-makers with a transparent tool for evaluating FCO to inform big-picture policy decisions [52]. Nuclear fuel cycle simulators were initially introduced by the Nuclear Strategy Project at Science Applications International Corp to provide simple system dynamic models to improve technical dialog between policymakers and expert groups [52]. Since then, national laboratories around the globe have driven development of nuclear fuel cycle simulators. These simulators track the flow of materials through the nuclear fuel cycle, from enrichment to final disposal of the fuel. However many have been developed for customized applications, resulting in inflexible architectures [23].

Two methods can be used to model facility and material flow in nuclear fuel cycle simulators: fleet-level and agent-level. Fleet-based models do not distinguish between discrete facilities or materials but instead lump them into fleets and streams but they offer simplicity and lower comput-

Table 2.1: Nuclear fuel cycle simulator tools and their corresponding organizations.

NFC Simulator	Country	Organization(s) associated with it
ANICCA [45]	Belgium	Studiecentrum voor Kernenergie (SCK CEN)
CAFCA [19]	USA	Massachusetts Institute of Technology (MIT)
CLASS [33]	France	Le Centre National De La Recherche Scientifique (CNRS), Institute for Radiological Protection and Nuclear Safety (IRSN)
COSI [11]	France	Commissariat à l'Énergie Atomique et aux Énergies Alternatives (CEA)
CYCLUS [23]	USA	University of Wisconsin (UW), University of Illinois at Urbana-Champaign (UIUC)
DESAE [49]	-	Organisation for Economic Co-operation and Development (OECD)
DYMOND [52]	USA	Argonne National Laboratory (ANL)
EVOLCODE2 [55]	Spain	Centro de Investigaciones Energéticas, Medioambientales y Tecnológicas (CIEMAT)
FAMILY21 [30]	Japan	Japanese Atomic Energy Agency (JAEA)
MARKAL [15]	USA	Brookhaven National Laboratory (BNL)
NFCSim [41]	USA	Los Alamos National Laboratory (LANL)
NFCSS [25]	-	International Atomic Energy Agency (IAEA)
ORION [17]	UK	National Nuclear Laboratory (NNL)
VISION [28]	USA	Idaho National Laboratory (INL)

tational cost. Agent-based models treat facilities and materials as discrete objects. This method's advantages are more flexible simulation control, ease of simulating a wide range of scenarios with new technologies, enabling of plug-and-play comparison of modeling methodologies, and allowing for a range of fidelities. Many nuclear fuel cycle simulators value integral effects over isotopic and facility-level resolution by modeling only fleet-level dynamics, grouping facilities into fleets and materials into streams [23].

Historically, national laboratories have restricted public access to their tools, resulting in universities and other non-laboratory organizations creating their own nuclear fuel cycle simulator tools. Table 2.1 shows a breakdown of all major nuclear fuel cycle simulators and the organization(s) associated with them.

In this work, we use the CYCLUS and DYMOND nuclear fuel cycle simulator tools. The CYCLUS nuclear fuel cycle simulator was created to break the practice of tools with inflexible architectures and restricted access [23]. CYCLUS is an open source nuclear fuel cycle simulator with agent-based modeling of discrete facilities and isotopic materials. With an agent-based framework, the

simulator tracks transformation and trade of resources between agents with customizable behavior [23]. This enables extension and reuse of this tool for fuel cycle simulations with different objectives. DYMOND is a hybrid nuclear fuel cycle simulator tool that uses fleet-based modeling for all facilities and materials with an exception of discrete modeling for reactor facilities. Chapter 3 provides more detail about CYCLUS and DYMOND.

## 2.2 Transition Scenario Capabilities in Nuclear Fuel Cycle Simulators

The Office of Nuclear Energy’s FCO Campaign led an evaluation and screening study of a comprehensive set of nuclear FCOs to identify FCOs with the potential to substantially improve the nuclear fuel cycle in the challenge areas [51]. The evaluation and screening study identified 40 Evaluation Groups (EGs) to represent a comprehensive set of all possible nuclear fuel cycles [51]. Each evaluation group consists of a group nuclear fuel cycles that similar resource requirements, fuel mass usage and compositions, and disposal needs [51]. The study assessed each evaluation group using 9 evaluation criteria: nuclear waste management, proliferation risk, nuclear material security risk, safety, environmental impact, resource utilization, development and deployment risk, institutional issues, and financial risk. The study concluded that fuel cycles involving continuous recycling of co-extracted U/Pu or U/TRU in fast spectrum critical reactors consistently scored high overall performance. EG23, EG24, EG29, and EG30 are the high-performing fuel cycle options [51]. These evaluation groups were evaluated at an equilibrium state to understand their end-state benefits. Knowing the most promising end-state evaluation groups, the next step is to evaluate and compare the transition process from the current EG01 state to these promising evaluation groups [14].

The transition from the once-through fuel cycle to a closed fuel cycle has a slow dynamic, and a complex interdependence of many factors. Thus, the study of transition scenarios using a nuclear fuel cycle simulator is key to understanding the influence of these multi-coupled factors on the transition. The U.S. national laboratories conducted a benchmarking effort of transition scenario capabilities in nuclear fuel cycle simulators [14, 18]. This comparison study aims to drive nuclear

fuel cycle simulator advancements and build confidence in the use of nuclear fuel cycle simulators in strategic and policy decisions [14].

Both nuclear fuel cycle simulator tools used in this thesis, CYCLUS and DYMOND, were verified in a transition scenario benchmarking effort [14, 4]. The reference problem used in the benchmark was a simplified transition from a one hundred 1000-MWe LWRs to a 333.3-MWe SFR fleet. They were found to have excellent agreement with the analytical solution and other nuclear fuel cycle simulators, ORION, VISION, and MARKAL. This benchmarking effort proved that these nuclear fuel cycle simulators are capable of simulating a simple transition scenario. However, to evaluate the nuclear fuel cycle simulators' flexibility, Feng et al concluded that more efforts must be made to model realistic transition scenarios [14].

## 2.3 Sensitivity Analysis Studies

We simulate transition scenarios to predict the future; however, when implemented in the real world, the simulated scenarios tend to deviate from the optimal scenario. Also, transition scenario analysis using nuclear fuel cycle simulators are imperfect representations of the real world [1]. Therefore, sensitivity analysis studies of nuclear fuel cycle transition scenarios must be conducted to better understand the impact of the variation of input parameters on performance metrics, enabling the nuclear fuel cycle simulators to more reliably inform policy decisions [36].

Transition scenario sensitivity analysis is a technique used to determine how varying different input variables impacts a transition scenario's performance metrics. Assumptions about facility parameters and technology readiness are made when setting up the simulation scenarios. Sensitivity analysis evaluates each performance metric's sensitivity to each assumption. Previous work towards sensitivity analysis and uncertainty quantification of nuclear fuel cycle simulations used these terms interchangeably because uncertainty quantification is viewed as design uncertainty [1]. For example, a never-been-built pyrochemical reprocessing facility's throughput is viewed as a variable design parameter. We determine how variation of the pyroprocessing facility's throughput impacts performance metrics. Therefore, in this thesis, we refer to both sensitivity analysis and uncertainty quantification as sensitivity analysis. By conducting studies on an extensive input parameter set, it is possible to determine the input parameters' that each performance metric is

most sensitive to. This helps us target where we should conduct closer sensitivity analysis and add further modeling detail. It also identifies which parameters the system is relatively insensitive to [1].

In this work, we use three types of sensitivity analysis: one-at-a-time, synergistic, and global.

### 2.3.1 One-at-a-time Sensitivity Analysis

The one-at-a-time sensitivity analysis technique estimates the isolated effect of one input variable. This approach gives each variable's local impact on the performance metrics. OECD conducted an one-at-a-time sensitivity analysis [1] on key nuclear fuel cycle input parameters and quantified the impacts on the performance metrics. In the OECD study, the base scenario used has a duration of 200 years and begins with Pressurized Water Reactors (PWRs), that transition to SFRs while maintaining constant electricity production. Each parameter was varied independently for three cases: the base case, a high case, and a low case with respect to the base case. The results of these variations on the performance metrics are expressed in tornado plots and sensitivity tables. The OECD study's analysis overview is given in Figure 2.1. Figure 2.2 shows an example tornado plot from the OECD study that represents the sensitivity of the separated Pu in storage amount to the various input parameters.

### 2.3.2 Synergistic Sensitivity Analysis

The synergistic sensitivity analysis technique involves multi-parameter input sweeps to view how synergistically changing input variables impacts the performance metrics. Synergistic sensitivity analysis is conducted by varying two input variables simultaneously and viewing their combined impact on each performance metric or a combination of weighted performance metrics. Passerini et al [36] applied this analysis method on nuclear fuel cycle simulations. Figure 2.3 shows the results of a synergistic analysis conducted by Passerini et al [36] in which thermal reprocessing and fast reactor technology introduction dates were varied. The plot shows an objective payoff surface representing a combination of weighted optimization criteria: minimize construction of reprocessing plants, minimize LCOE, minimize depleted uranium generated, and minimize total SWU used. This type of synergistic studies successfully informs on how variation in two input

S $(r^2 \geq 0,9)$	PWR cycle			FR cycle			Reprocessing	Inventory								
	Front-end		Back-end	Front-end		Back-end		Pu			Reactors			Storages		
	Uranium	Enrichment	Fabrication	Storage	Pu	Fabrication	Storage	PWR	FR	Plants	Cycle	Waste	Cycle	Waste		
<b>Reactor characteristics</b>																
Breeding gain	?				?					?			?	?	?	?
Reactor Lifetime							?									
<b>MA Recycling</b>																
MA content																
MA recuperation rate																
<b>General Scenario Assumption</b>																
Energetic production									?					?		
Minimum cooling time	PWR															
	FR															
Fabrication time	PWR															
	FR															
Introduction date of FR																
Rate of introduction																
<b>Reprocessing</b>																
First year of reprocessing	PWR				?								?	?		?
	FR							?		?			?	?	?	?
Reprocessing capacity	PWR			?									?	?		
	FR							?		?			?	?	?	?
(U, Pu) Losses	?						?		?							
Enrichment tail		?														
<b>Sensitivity Coefficients</b>																
	$\leq -1$										$\geq +1$					

Figure 2.1: Overall results from OECD one-at-a-time sensitivity analysis study. This is reproduced from the OECD report [1]. Sensitivity Table with an overview of all the sensitivity indicators S obtained from the various input parameters (one row for each input parameter) and the various output parameters (one column for each output parameter). When a sensitivity coefficient is positive (red), this means an increase of the input parameter induces an increase of the output parameter. Whereas, when it is blue, this means an increase of the input parameter induces a decrease of the output parameter. When a coefficient of determination  $r^2$  is lower than 0.9, then the related sensitivity indicator is replaced by a question mark ? in the table. When the output parameter is not impacted by the variation of the input parameter, then the related sensitivity indicator is not available and it is replaced by a blank in the table. [1].

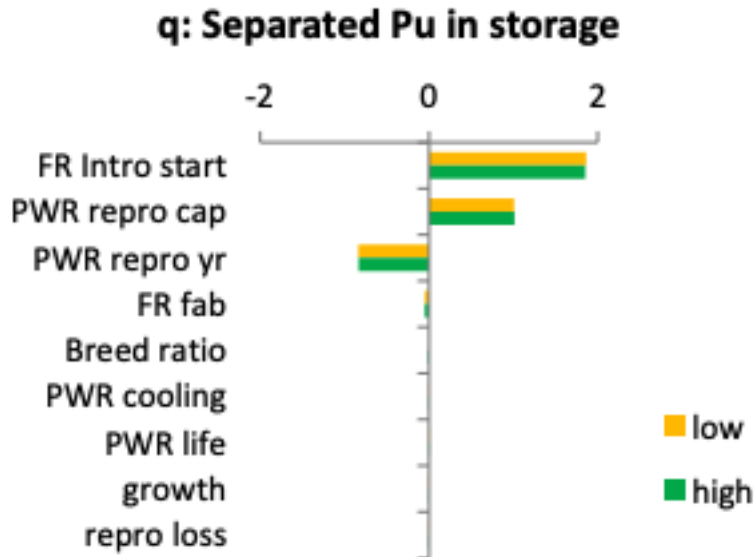


Figure 2.2: A tornado plot from the OECD one-at-a-time sensitivity analysis study, showing the sensitivity of the separated Pu in storage amount to each input parameter. This is reproduced from the OECD report [1].

variables impacts the system; however, if more than two input variables are varied, it is difficult to visualize the impact on the system in a plot. Therefore, the subsequent section’s global sensitivity analysis method is introduced to inform on the global sensitivity of the system.

### 2.3.3 Global Sensitivity Analysis

To fully consider the synergistic effects of simultaneous variation of all the nuclear fuel cycle input parameters, a variance-based approach can be used instead [48]. Thiolliere et al. conducted a global sensitivity analysis of a nuclear fuel cycle transition scenario by using Latin Hypercube sampling [47] to generate Sobol indices [31] that indicate which design parameters have the most influence on the performance metrics. They applied this method to a simplified PWR UOX and PWR MOX fleet. Latin Hypercube sampling is a statistical method for generating random samples of parameter values from a multidimensional distribution. For Latin Hypercube Sampling of M input parameters, the user first chooses the number of sample points, N, then each parameter’s input space is divided into N sub-sections. The algorithm will then select a random value from each sub-section for each input parameter. Once there is a list of samples for each input parameter, they

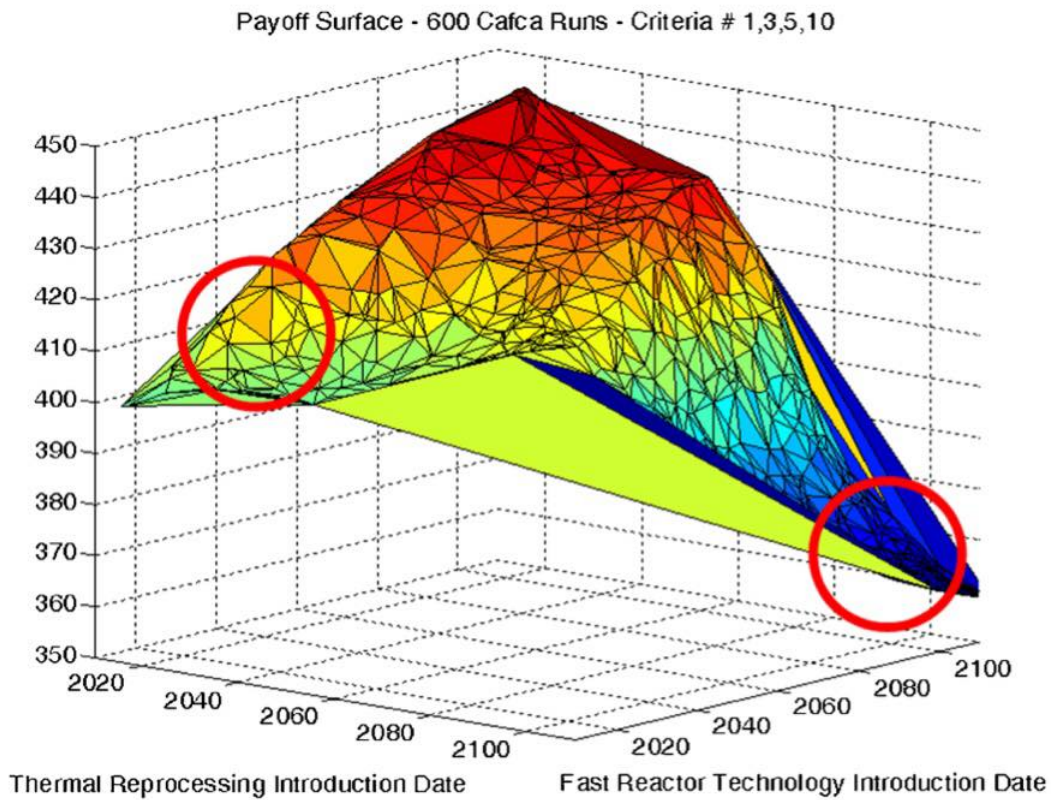


Figure 2.3: Payoff surface for variation in thermal reprocessing and fast reactor technology introduction date [36]. The payoff surface represents a combination of weighted optimization criteria: minimize construction of reprocessing plants, minimize LCOE, minimize depleted uranium generated, and minimize total SWU used.

are combined randomly to form M-dimensional sets [47]. The nuclear fuel cycle simulation is run M times and the performance metrics of interest are recorded. Sobol sensitivity analysis provides how much variability in the model's performance metrics is dependent on each input parameter [54]. Sobol Indices decomposes the variance of the metric into fractions attributed to inputs or sets of inputs. A large Sobol index signifies that variation in that input variable is more impactful to the output parameter. A model is viewed as a function:

$$Y = f(\mathbf{X})$$

where:

$Y$  = Performance metric

$\mathbf{X}$  = vector of  $d$  input parameters

$d$  = No. of varying input parameters

First order Sobol indices measure the effect of one input parameter on the performance metric with an average over variations in other input parameters [26]:

$$S_i = \frac{V_i}{Var(Y)}$$

where:

$S_i$  = First order sensitivity index

$V_i = Var_{X_i}(E_{\mathbf{X}(\sim i)}(Y|X_i))$  = Conditional variance

$\mathbf{X}(\sim i)$  = the set of all variables except  $X_i$

Total-effect Sobol indices measure the effect of the first order Sobol index plus all the interactions the one input parameter has with other input parameters [21]:

$$S_{Ti} = 1 - Var_{\mathbf{X}(\sim i)}(E_{X_i}(Y|\mathbf{X}(\sim i)))$$

#### **2.3.4 Summary of Sensitivity Analysis Studies**

Sensitivity analysis studies of nuclear fuel cycles have previously been used to narrow down and compare a wide range of nuclear fuel cycle scenarios to determine the ideal scenario. The evaluation and screening study [51] determined that the desired fuel cycle end states were fuel cycles involving continuous recycling of co-extracted U/Pu or U/TRU in fast spectrum critical reactors. These evaluation and screening study's sensitivity analysis focused on macro-level input parameters such as types of reactor and reprocessing technologies. However, sensitivity analyses regarding dynamic nuclear fuel cycle transitions are rare. The only relevant sensitivity study was conducted by OECD [1], however it was a basic one-at-a-time sensitivity analysis. Therefore, synergistic and global sensitivity analysis studies focused on micro-level input parameters such as length of cooling time and introduction date of reprocessing/reactor technologies, should be conducted to understand how their variation impacts the performance metrics. Using the sensitivity analysis results, these transition scenarios can be further optimized and used to inform other nuclear research areas. For example, by studying how the throughput of a reprocessing facility impacts the performance metrics, we can determine the ideal reprocessing facility size.

# Chapter 3

## Methods

In this chapter, we describe the nuclear fuel cycle simulators utilized in this work, CYCLUS and DYMOND, and the new capabilities developed for them. The new capabilities developed are:

1. Demand-driven deployment in CYCLUS.
2. Sensitivity analysis for DYMOND.
3. Sensitivity analysis for CYCLUS.

### 3.1 Cyclus

In this section, we describe CYCLUS, a nuclear fuel cycle simulator. In CYCLUS, an agent-based nuclear fuel cycle simulation framework [23], each entity (i.e. `Region`, `Institution`, or `Facility`) in the fuel cycle is an agent. `Region` agents represent geographical or political areas in which `Institution` and `Facility` agents reside. `Institution` agents represent legal operating organizations such as utilities, governments, and control the deployment and decommissioning of `Facility` agents [23]. `Facility` agents represent nuclear fuel cycle facilities such as mines, conversion facilities, reactors, reprocessing facilities, etc. Figure 3.1 illustrates CYCLUS’ modular architecture in which user-selected archetypes are loaded into the simulation. CYCMORE [6] provides basic `Region`, `Institution`, and `Facility` archetypes compatible with CYCLUS. CYCLUS records isotopic mass flows and inventories at an agent level.

Two of CYCLUS’ main design objectives are user customization and extensibility. CYCLUS’ modularity, open architecture, and agent interchangeability achieve these objectives. The modularity and open architecture provide users with a platform to develop custom facilities with their chosen fidelity and capabilities. Agent interchangeability facilitates the configuration of custom fuel cycles

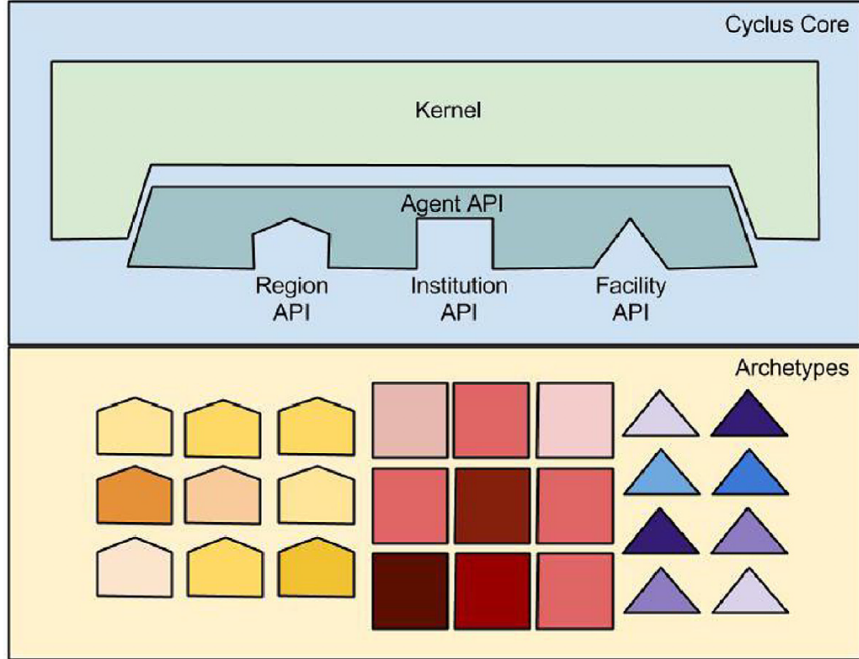


Figure 3.1: The CYCLUS core provides an application programming interface (API) to modularly load user-selected archetypes into the CYCLUS simulation [23].

and direct comparisons of alternative modeling methodologies and facility concepts [23]. CYCLUS' input file has an XML or JSON format, and the output file is a SQLite or HDF5 database.

CYCLUS' agent-based modeling, modular architecture, and flexible extendability make it a one-of-a-kind fuel cycle simulator since most fuel cycle simulators (Table 2.1) have inflexible architectures and use fleet-based modeling. Therefore, it is straightforward to introduce a **CYCLUS Institution** agent to enable demand-driven deployment of reactor and supporting fuel cycle facilities.

### 3.2 Demand driven deployment capability in Cyclus (d3ploy)

In 2016, a DOE initiative sought to understand and evaluate the transition from the current once through LWR fuel cycle (EG01) to promising future nuclear fuel cycles [14]. In CYCLUS, reactor facilities are automatically deployed to meet user-defined power demand. However, the user is required to define a deployment scheme for all supporting facilities to avoid any supply chain gaps or resulting idle reactor capacity. To avoid this issue, users must set infinite capacities for the support facilities, but this inaccurately represents reality and obfuscates required capacities. Manually

determining a deployment scheme for a once-through fuel cycle is straightforward, however, for complex fuel cycle scenarios, it is not. To ease setting up realistic nuclear fuel cycle simulations, a nuclear fuel cycle simulator must bring dynamic demand-responsive deployment decisions into the simulation logic [22]. This means the nuclear fuel cycle simulator decides how many mines, mills, enrichment facilities, reprocessing facilities, etc are deployed to support dynamically changing power demand and reactor types. Thus, a next-generation nuclear fuel cycle simulator must predictively and automatically deploy fuel cycle facilities to meet a user-defined power demand. Therefore, the Demand-Driven Cycamore Archetypes project (NEUP-FY16-10512) was initiated to develop demand-driven deployment capabilities in CYCLUS. This capability, `d3ploy`, is a CYCLUS **Institution** agent that deploys facilities to meet user-defined power demand.

### 3.2.1 `d3ploy` framework

`d3ploy` was developed collaboratively with contributors from both UIUC and University of South Carolina (USC). A breakdown of contributions can be viewed at the `d3ploy` github repository [3].

In CYCLUS, developers have the option to design agents using C++ or Python. The `d3ploy` **Institution** agent was implemented in Python to enable the use of well-developed time series forecasting Python packages.

In a CYCLUS simulation, at every time step, `d3ploy` predicts the supply and demand of each commodity for the next time step. Commodities refer to materials in the nuclear fuel cycle such as reactor fuel. Upon undersupply for any commodity, `d3ploy` deploys facilities to meet its predicted demand. Therefore, if the simulation begins with user-defined power demand, `d3ploy` deploys reactors to meet power demand, followed by enrichment facilities to meet fuel demand, and so on, to create the supply chain. Based on the demand and supply trends of each commodity, `d3ploy` predicts their future demand and supply, and deploys facilities accordingly to meet the future demand to prevent demand from surpassing supply. Figure 3.2 shows the logical flow of `d3ploy` at every time step. In subsequent subsections, we describe how to set up a transition scenario using `d3ploy` and the input parameters `d3ploy` accepts.

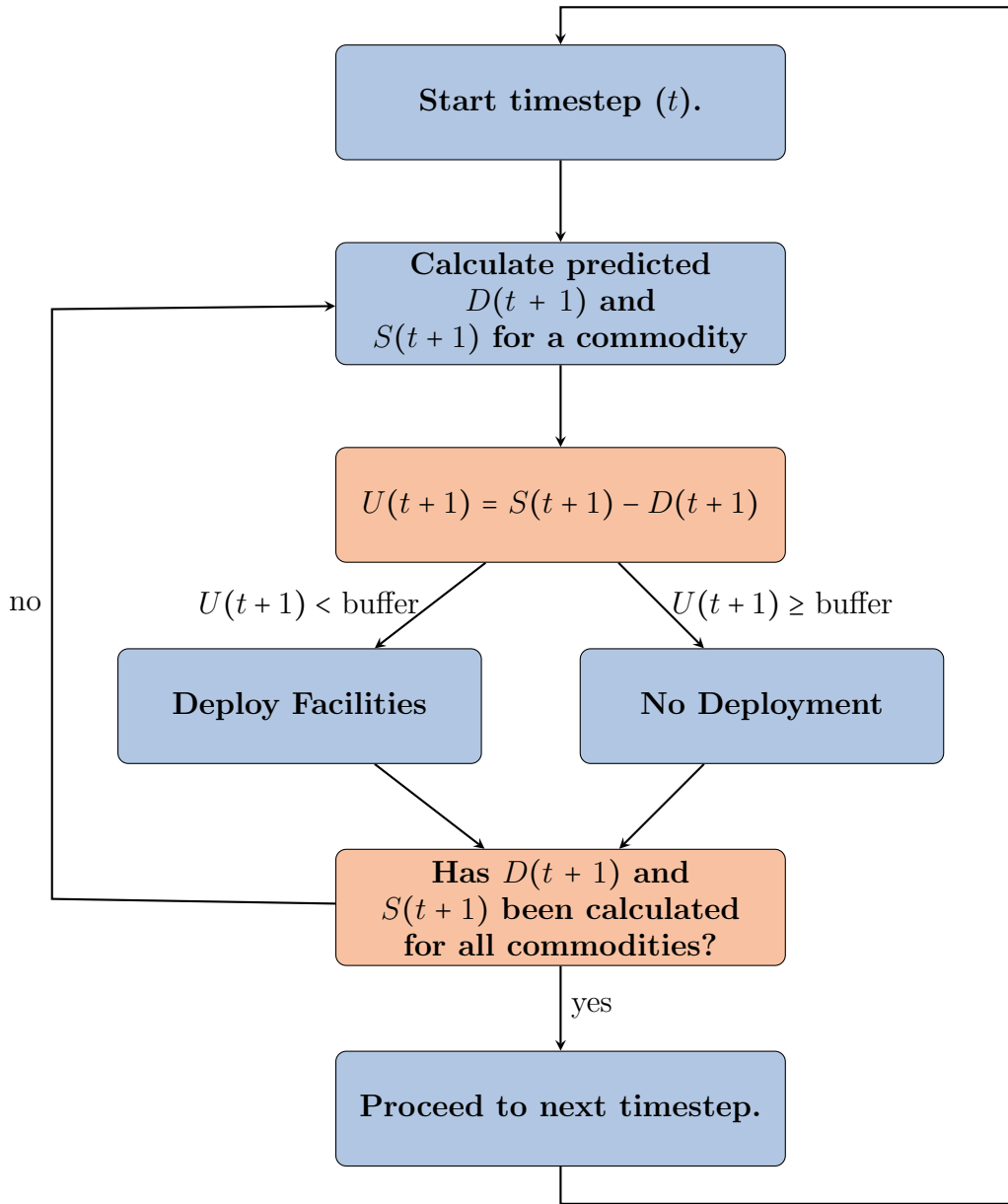


Figure 3.2: `d3ploy` logic flow at every timestep in CYCLUS [8].

`d3ploy` aims to minimize the undersupply of power:

$$obj = \min \sum_{t=1}^{t_f} |D_{t,p} - S_{t,p}|. \quad (3.1)$$

where:

$t_f$  = Number of time steps [months]

$t$  = time [month]

$D$  = Demand

$S$  = Supply

$p$  = power [MW]

The sub-objectives are to minimize the number of time steps of undersupply or under-capacity of any commodity:

$$obj = \min \sum_{c=1}^M \sum_{t=1}^{t_f} |D_{t,c} - S_{t,c}|, \quad (3.2)$$

and to minimize excessive oversupply of all commodities:

$$obj = \min \sum_{c=1}^M \sum_{t=1}^{t_f} |S_{t,c} - D_{t,c}|. \quad (3.3)$$

where:

$c$  = commodity type

$M$  = Number of commodities

Minimizing excessive oversupply reflects reality, in which utilities ensure grid availability by ensuring power plants are never short of fuel while avoiding expensive storage of excess fuel. Nuclear fuel cycle simulations often face power shortages due to lack of viable fuel, despite having sufficient installed reactor capacity. Using `d3ploy` to automate the deployment of supporting facilities

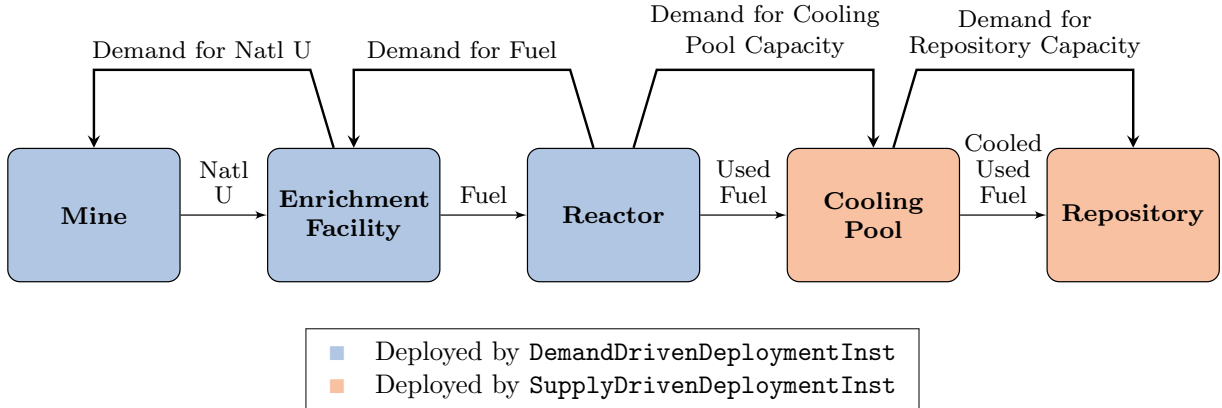


Figure 3.3: Simple once-through fuel cycle depicting which facilities are deployed by `DemandDrivenDeploymentInst` and `SupplyDrivenDeploymentInst`.

prevents this.

## Structure

Front-end facilities meet the demand for commodities they produce, whereas back-end facilities meet supply for the commodities they demand. Therefore, in `d3ploy` two distinct institutions control front-end and back-end fuel cycle facilities: `DemandDrivenDeploymentInst` and `SupplyDrivenDeploymentInst`, respectively. For example, when a reactor facility demands fuel, `DemandDrivenDeploymentInst` deploys fuel fabrication facilities to create fuel supply. For back-end facilities, the reactor generates spent fuel, and `SupplyDrivenDeploymentInst` deploys used fuel storage facilities to create capacity to store the spent fuel. Figure 3.3 depicts a simple once-through fuel cycle and the `Institution` type governing each facility's deployment.

## Deployment-Driving Method

To prevent over-deployment of facilities with an intermittent supply such as reactors that require refueling, and to prevent infinite deployment of a facility that demands a commodity no longer available in the simulation, we introduced the capability to deploy facilities based on the difference between predicted demand and installed capacity. The user may deploy facilities based on the difference between predicted demand and predicted supply, *or* predicted demand and installed capacity. For example, a reprocessing plant that fabricates Sodium-Cooled Fast Reactor (SFR) fuel demands for Pu after depletion of the existing Pu inventory and decommissioning of the LWR

reactors that produce it. If we used the deployment-driving method driven by the difference in predicted demand and predicted supply, this results in infinite deployment of reprocessing facilities in a futile attempt to produce SFR fuel, crashing the simulation. Instead, if we use the deployment-driving method driven by the difference in predicted demand and installed capacity, only one reprocessing facility will be deployed, the simulation will finish, and the user will see that a large Pu inventory must be accumulated. Therefore, using the deployment-driving method that deploys facilities based on the difference between predicted demand and installed capacity is ideal for most transition scenarios.

## Input Variables

Table 3.1 lists and gives examples of the input variables `d3ploy` accepts. The user must define the following input variables:

- **available facilities for `d3ploy` to deploy in the simulation and their respective capacities.** The user must define the facilities he/she wants `d3ploy` to deploy. It is the user's responsibility to ensure the defined facilities create a supply chain to produce the demand driving commodity.
- **the demand driving commodity and its demand equation.** For most simulations, the demand driving commodity is power. The demand equation is defined by a mathematical equation with units of MW. For example, a constant power demand equation is 10000, while a linearly increasing power demand equation is  $100t$ .
- **the deployment driving method.** This input variable is described above.
- **the prediction method.** This input variable is described below.

There are also optional input variables:

- **supply/capacity buffers for individual commodities.** This input variable is described below.
- **facility preferences.** This input variable is described below.
- **facility fleet shares.** This input variable is described below.

Table 3.1: d3ploy's required and optional input parameters with examples.

	<b>Input Parameter</b>	<b>Examples</b>
<b>Required</b>	Demand driving commodity	Power
	Demand equation [MW]	$P(t) = 10000, \sin(t), 10000t$
	Available Facilities	Mine, LWR reactor, Repository, etc.
	Capacities of the facilities	3000 kg, 1000 MW, 50000 kg
		Power: fast fourier transform
	Prediction method	Fuel: moving average Spent fuel: moving average
	Deployment driven by	Installed Capacity
<b>Optional</b>	Supply/Capacity Buffer type	Absolute
		Power: 3000 MW
	Supply/Capacity Buffer size	Fuel: 0 kg Spent fuel: 0 kg
	Facility preferences [month]	LWR reactor = 100-t SFR reactor = t-99
	Fleet share percentage [%]	MOX LWR = 85% SFR = 15%

## Supply/Capacity Buffer

The user has the option to specify a supply buffer for each commodity; d3ploy accounts for the buffer when calculating predicted demand and deploys facilities accordingly. The buffer is defined as a percentage:

$$S_{pwb} = S_p(1 + d) \quad (3.4)$$

or absolute value:

$$S_{pwb} = S_p + b \quad (3.5)$$

where:

$S_{pwb}$  = predicted supply/capacity with buffer

$S_p$  = predicted supply/capacity

$d$  = buffer's percentage value in decimal form

$b$  = buffer's absolute value

Using the buffer capability and installed capacity to drive facility deployment in a transition scenario simulation will effectively minimize undersupply of a commodity while avoiding excessive oversupply. This is demonstrated in Section 4.1.

## Facility Preference and Fleet Share

The user can define time-dependent preference equations to facilities' that supply the same commodity. If there are two reactor types, LWRs and SFRs, in a simulation, the user can make use of time-dependent preferences to make the simulation deploy LWRs at earlier times in the simulation, and deploy SFRs at later times in the simulation when there is a power demand. In Table 3.1, the user defined that the LWR has a preference of  $100 - t$ , while the SFR has a preference of  $t - 99$ . Figure 3.4 depicts how the preference for each reactor changes with time. When there is a power

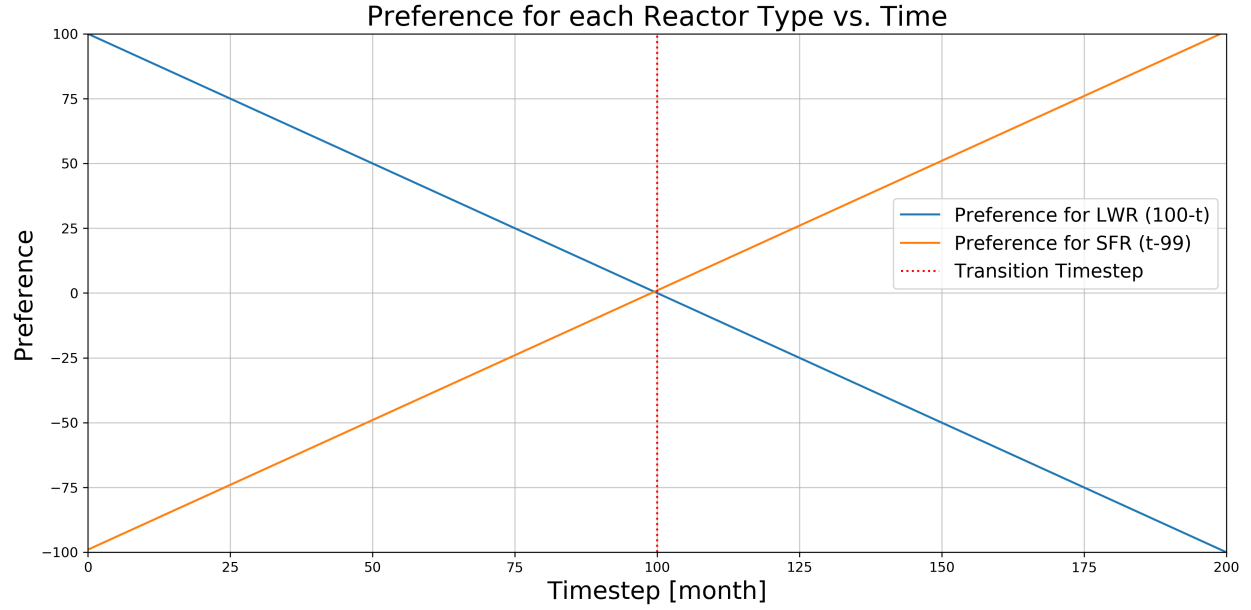


Figure 3.4: `d3ploy` has a  $100 - t$  preference for LWRs and a  $t - 99$  preference for SFRs. When there is a power undersupply, `d3ploy` will deploy the reactor that has a larger preference at that time step.

undersupply, `d3ploy` will deploy the reactor that has a larger preference at that time step. At time step 100, LWR preference is 0, while SFR preference is 1; therefore a SFR is deployed if there is a power shortage. Thus, the transition occurs at the 100<sup>th</sup> time step.

The user also has the option to specify fleet-share for facilities that provide the same commodity. For example, if there are two reactor types, mixed oxide (MOX) LWRs and SFRs, in a simulation, the user can make use of fleet-share specifications to determine the percentage of power supplied by each reactor. When MOX LWR has a share of  $s\%$  and SFR has a share of  $(100 - s)\%$ , MOX LWR deployment constrains to  $s\%$  of total power demand and SFR deployment constrains to  $(100 - s)\%$  of total power demand.

The transition year is selected by customizing facility preferences to prefer advanced reactors at that year. The fleet-share percentage determines the share of each type of reactor to transition to. Figure 3.5 shows the logical flow of which facility `d3ploy` deploys when there are multiple facilities offering the same commodity.

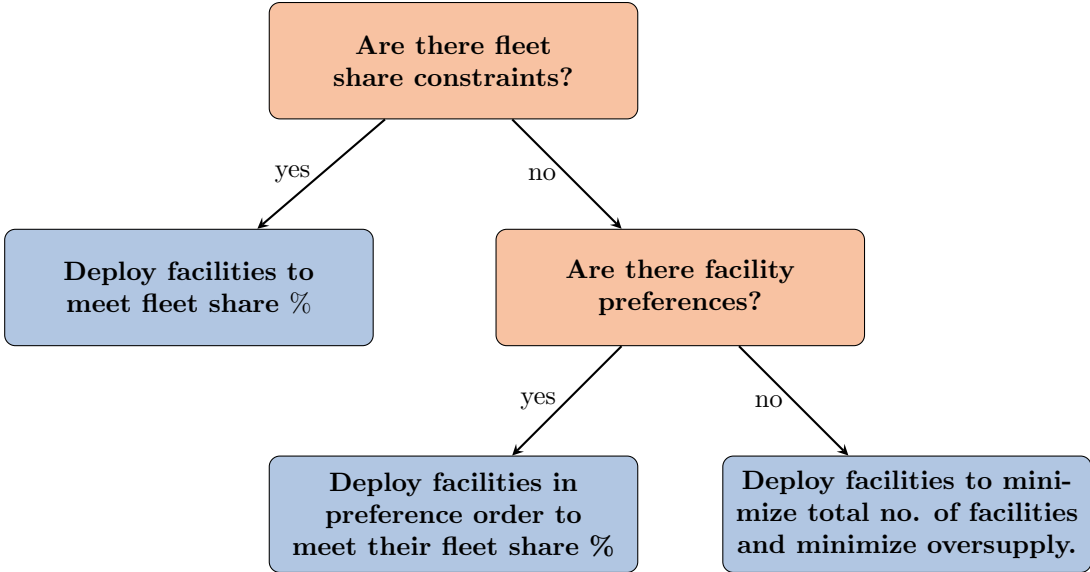


Figure 3.5: Logical flow of how d3ploy selects which facility to deploy when there are multiple facilities offering the same commodity.

## Prediction Methods

d3ploy records supply and demand at each time step for all commodities. Time-series data informs d3ploy’s time series forecasting methods which predict future supply and demand for each commodity. The time series forecasting methods investigated include non-optimizing, deterministic-optimizing, and stochastic-optimizing methods. Non-optimizing methods are techniques that harness simple moving average and autoregression concepts which use historical data to infer future supply and demand values. Deterministic-optimizing and stochastic-optimizing methods are techniques that use an assortment of more sophisticated time series forecasting concepts to predict future supply and demand values. Deterministic-optimizing methods give deterministic solutions, while stochastic-optimizing methods give stochastic solutions.

Depending on the scenario in question, each forecasting method offers distinct benefits and disadvantages. The various methods are compared for each type of simulation to determine the most effective prediction method for a given scenario. The following sections describe the prediction methods.

### *Non-Optimizing Methods*

Non-optimizing methods include: Moving Average (MA), Autoregressive Moving Average (ARMA), and Autoregressive Heteroskedasticity (ARCH). The MA method calculates the average of a user-

defined number of previous entries in a commodity's time series and returns it as the predicted value:

$$\text{Predicted Value} = \frac{\sum_{n=1}^N V_n}{n}. \quad (3.6)$$

where:

$V_n$  = Time series value

$N$  = length of timeseries

The ARMA method combines moving average and autoregressive models (equation 3.7), and is used to describe a time series in terms of moving average and autoregression polynomials [37]. The first term is a constant, second term is white noise, the third term is the autoregressive model, and the fourth term is the moving average model. The ARMA method is more accurate than the MA method because of the inclusion of the autoregressive term:

$$X_t = c + \epsilon_t + \sum_{i=1}^p \varphi_i X_{t-i} + \sum_{i=1}^q \theta_i \epsilon_{t-i}. \quad (3.7)$$

where:

$c$  = a constant

$\epsilon_t$  = error terms (white noise)

$\varphi$  = the autoregressive models parameters

$\theta$  = the moving average models parameters

$p$  = order of the autoregressive polynomial

$q$  = order of the moving average polynomial

The ARCH method models time series data by describing the variance of the current error term

as a function of the sizes of the previous time periods' error terms [13]. This allows the method to support changes in the time dependent volatility, such as increasing and decreasing volatility in the same series [13]. The **ARCH** method is better than the **ARMA** method for volatile time-series data [16]. The StatsModels [43] Python package is used to implement **ARMA** and **ARCH** methods in **d3ploy**.

#### *Deterministic-Optimizing Methods*

Deterministic methods include Fast Fourier Transform (**FFT**), Polynomial Fit (**POLY**), Exponential Smoothing (**EXP-SMOOTHING**), and Triple Exponential Smoothing (**HOLT-WINTERS**). The **FFT** method uses the fast fourier transform algorithm to map a time series into the frequency domain. The algorithm returns complex numbers from which frequency, amplitude, and phase is extracted. Future demand and supply values are predicted by summing the significant components, then using the inverse fourier transform method to return it into a usable form. The discrete fourier transform (**DFT**) transforms a sequence of N complex numbers ( $X_k$ ) into another sequence of complex numbers ( $x_n$ ) [39]:

$$X_k = \sum_{n=0}^{N-1} x_n e^{-i2\pi kn/N}. \quad (3.8)$$

where:

$X$  = sequence of complex numbers

$k = 0, \dots, N - 1$

$N$  = No. of complex numbers

$x$  = sequence of complex numbers

$n = 0, \dots, N - 1$

This method is implemented in **d3ploy** using the SciPy [29] Python package.

The **POLY** method fits the time series data with a user-defined  $n^{th}$  degree polynomial and uses the fitted trend-line to determine future demand and supply values:

$$Y_t = \beta_0 + \sum_{n=1}^N \beta_n t^n + \varepsilon \quad (3.9)$$

where:

$t$  = time index

$n$  = polynomial order

$\beta$  = fitted parameters

This method was implemented in `d3ploy` using the NumPy [35] Python package. The **EXP-SMOOTHING** and **HOLT-WINTERS** methods use a weighted average of time-series data with exponentially decaying weights for older time series values [24] to create a model to determine future demand and supply values. The **EXP-SMOOTHING** method excels in modeling univariate time series data without trend or seasonality [24]:

$$y_{t+1} = \alpha y_t + (1 - \alpha) y_t. \quad (3.10)$$

where:

$y$  = timeseries value

$$\alpha = \text{smoothing factor } (0 < \alpha < 1) \quad (3.11)$$

The **HOLT-WINTERS** method applies triple exponential smoothing, resulting in higher accuracy when modeling seasonal time series data [44]:

$$\begin{aligned}
F_{t+m} &= (S_t + mb_t)I_{t-L+m} \\
S_t &= \alpha \frac{y_t}{I_{t-L}} + (1 - \alpha)(S_{t-1} + b_{t-1}) \\
b_t &= \gamma(S_t - S_{t-1}) + (1 - \gamma)b_{t-1} \\
I_t &= \beta \frac{y_t}{S_t} + (1 - \beta)I_{t-L}
\end{aligned} \tag{3.12}$$

where:

$F$  = forecast at m periods ahead

$t$  = time period index

$S$  = smoothed observation

$y$  = the observation

$b$  = trend factor

$I$  = seasonal index

$\alpha, \beta, \gamma$  = constants

The StatsModels [43] Python package was used to implement the EXP-SMOOTHING and HOLT-WINTERS methods in `d3ploy`.

#### *Stochastic-Optimizing Methods*

We implemented one stochastic-optimizing method: step-wise seasonal method (**SW-SEASONAL**). The method was implemented in `d3ploy` by the auto Auto-Regressive Integrated Moving Averages (ARIMA) method in the `pmdarima` [46] Python package. The ARIMA model is a dependent time series that is modeled as a linear combination of its own past values and past values of an error series [27]:

$$(1 - B)^d Y_t = \mu + \frac{\theta(B)}{\phi(B)} a_t \tag{3.13}$$

where:

$t$  = time index

$\mu$  = mean term

$B$  = backshift operator, such that  $BX_t = X_{t-1}$

$\phi(B)$  = autoregressive operator

$\theta(B)$  = moving average operator

$a_t$  = random error

### 3.3 DYMOND

DYMOND [52] is a nuclear fuel cycle simulator developed at Argonne National Laboratory (ANL). It is built using the AnyLogic simulation software with Microsoft Excel templates for data input and output. The primary inputs to this code are time-dependent power demand, reactor, and fuel cycle characteristics [14]. The code calls ORIGEN [5] during the simulation to conduct reactor depletion calculations. DYMOND records isotopic mass flows and inventories at a system-level. DYMOND's primary design objective is ease of understanding the simulator's behavior and variables.

In DYMOND, reactor facilities are automatically deployed to meet user-defined power demand, and the user can define the percentage share of energy for up to five reactor types. The user also defines the fuel loading model used to calculate reactor spent fuel compositions, the type of reprocessing technology for each reactor type, and the length of used fuel cooling time. In DYMOND, the user must define the deployment schedule for the reprocessing plants; the cooling pools and storage pools are all assumed to have infinite capacities. DYMOND does not have demand-driven deployment capabilities for supporting fuel cycle facilities.

The difference between CYCLUS and DYMOND is that CYCLUS uses agent-based modeling for all facilities and mass flows, whereas DYMOND uses fleet-based modeling for all facilities and mass flows except for reactor facilities. Compared to CYCLUS, DYMOND is easier to use but less flexible.

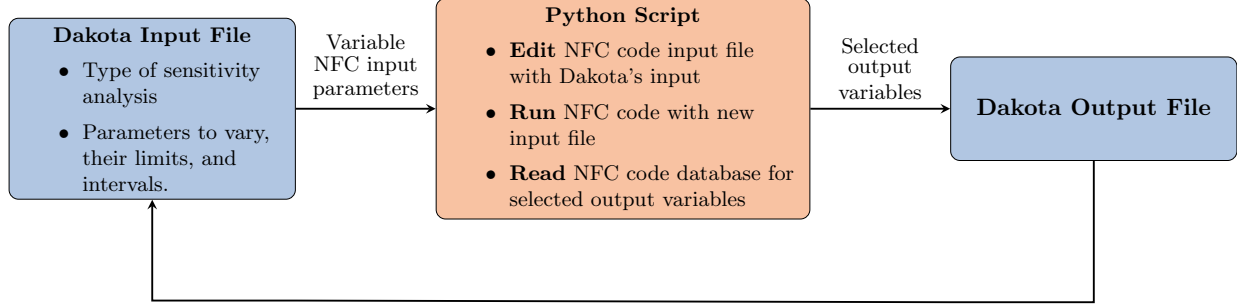


Figure 3.6: Depiction of the coupling of Dakota and each nuclear fuel cycle (NFC) code.

### 3.4 Sensitivity Analysis Capabilities

In this work, CYCLUS and DYMOND are coupled with Dakota [12] to give them sensitivity analysis, uncertainty quantification, and optimization capabilities. Dakota is a well supported sensitivity analysis, uncertainty quantification, and optimization tool that provides a flexible interface between analysis codes and iterative system analysis methods, created by Sandia National Laboratory (SNL) [50]. Other pieces of nuclear engineering software are coupled with Dakota to conduct sensitivity analysis [50, 53].

The process of coupling with Dakota is similar for both nuclear fuel cycle simulators. Figure 3.6 depicts the coupling; Dakota wraps each of the nuclear fuel cycle simulators. In this work, we developed the Python interface between Dakota and the nuclear fuel cycle simulators. The Python interface has three functions: (1) edit the nuclear fuel cycle simulator’s input file based on Dakota’s input values, (2) run the simulation with the newly edited nuclear fuel cycle simulator’s input file, and (3) read the nuclear fuel cycle simulator output file and returns values of interest to the Dakota output file. The Dakota input file defines the parameters for the sensitivity analysis, uncertainty quantification, or optimization study. The difference between the Python interface between CYCLUS-Dakota and DYMOND-Dakota is the methods used to read and write to their input and output files.

#### 3.4.1 DYMOND-Dakota Coupling (ddwrapper)

In the interface between DYMOND and Dakota, the Pywin32 [20] Python package is used to parse the Excel input file and to write to the relevant Excel cells accordingly. Pywin32 is a thin Python wrapper that enables interaction with COM objects [20]. The Pandas [32] Python package is used

to analyze the excel output database by taking the values of interest and formatting them to return to the Dakota output file. Scripts in the `ddwrapper` Github repository [7] demonstrate DYMOND and Dakota coupling.

### 3.4.2 Cyclus-Dakota Coupling (dcwrapper)

In the interface between CYCLUS and Dakota, the Jinja2 [40] Python package is used to edit the relevant parts of a CYCLUS XML input file. Jinja2 is a modern and designer-friendly templating language for Python. We use CYMETRIC to analyze CYCLUS' output database. CYMETRIC [42] is a general analysis library and tool created in 2015 to ease interaction with CYCLUS' SQL database. Scripts in the `dcwrapper` Github repository [10] demonstrate CYCLUS and Dakota coupling.

## 3.5 Chapter Summary

In this chapter, we introduced the nuclear fuel cycle simulators, CYCLUS and DYMOND. In CYCLUS, we implemented an `Institution`, `d3ploy`, that automatically deploys a supply chain of fuel cycle facilities to meet a user-defined power demand. We also coupled CYCLUS and DYMOND with Dakota, a sensitivity analysis tool. With these new capabilities, we use CYCLUS and DYMOND to conduct sensitivity analysis of transition scenario simulations. `d3ploy` will ensure automatic and effective transition set up in CYCLUS sensitivity analysis studies.

# Chapter 4

## Results: d3ploy Demonstration

In this chapter, we demonstrate `d3ploy`'s capabilities in CYCLUS transition scenario simulations.

This chapter has two sections:

1. `d3ploy` demonstration for simple three-facility transition scenarios
2. `d3ploy` demonstration for a complex closed cycle transition scenario

### 4.1 d3ploy Demonstration of Simple Transition Scenarios

This section demonstrates `d3ploy`'s capability to effectively set up a simple transition scenario simulation for constant, linearly increasing, and sinusoidal power demand simulations. These simulations are defined as *simple* since they only include three facility types: `source`, `reactor`, and `sink`. The simulations begin with ten `reactor` facilities (`reactor1` to `reactor10`). These reactors have staggered cycle lengths and lifetimes to prevent simultaneous refueling and to set up gradual decommissioning. `d3ploy` is configured to deploy `new reactor` facilities to meet the loss of power supply created by the decommissioning of the initial `reactor` facilities. Table 4.1 shows the `d3ploy` input parameters for these simulations. Figure 4.1 shows the user-defined power demand curves driving deployment in three simulations.

#### 4.1.1 Simple Transition Scenario Simulation: Constant Demand

Figures 4.2, 4.3a, and 4.3b demonstrate `d3ploy`'s capability to deploy reactor and supporting facilities to minimize undersupply when meeting constant power demand and subsequent secondary commodities demand. Table 4.2 shows the number of undersupplied timesteps. In Figure 4.2, there exist no time steps in which the supply of power falls under demand, meeting the main objective

Table 4.1: `d3ploy`'s input parameters for the simple constant, linearly increasing, and sinusoidal power demand transition scenarios.

Input Parameter	Simulation Description		
	Constant Power	Linearly Increasing Power	Sinusoidal Power
Demand driving commodity	Power		
Demand equation [MW]	10000	$t < 40: 10000$ $t \geq 40: 250t$	$10000 + 1000\sin(\pi * t/3)$
Available Facilities	Source, Reactor, Sink		
Prediction method	Power: FFT Fuel: MA Spent fuel: MA	Power: FFT Fuel: MA Spent fuel: FFT	Power: HW Fuel: MA Spent fuel: FFT
Deployment Driving Method	Installed Capacity		
Buffer type	Absolute		
Buffer size	Power: 3000 MW Fuel: 0 kg Spent fuel: 0 kg	Power: 2000 MW Fuel: 1000 kg Spent fuel: 0 kg	Power: 2000 MW Fuel: 1000 kg Spent fuel: 0 kg

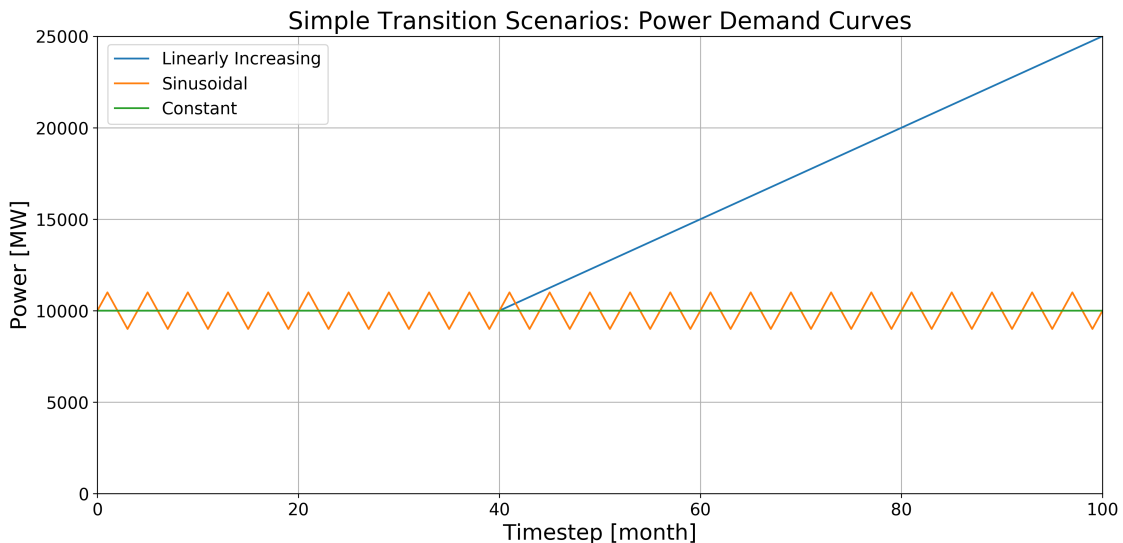


Figure 4.1: Power demand curves for the simple constant, linearly increasing, and sinusoidal power demand transition scenarios.

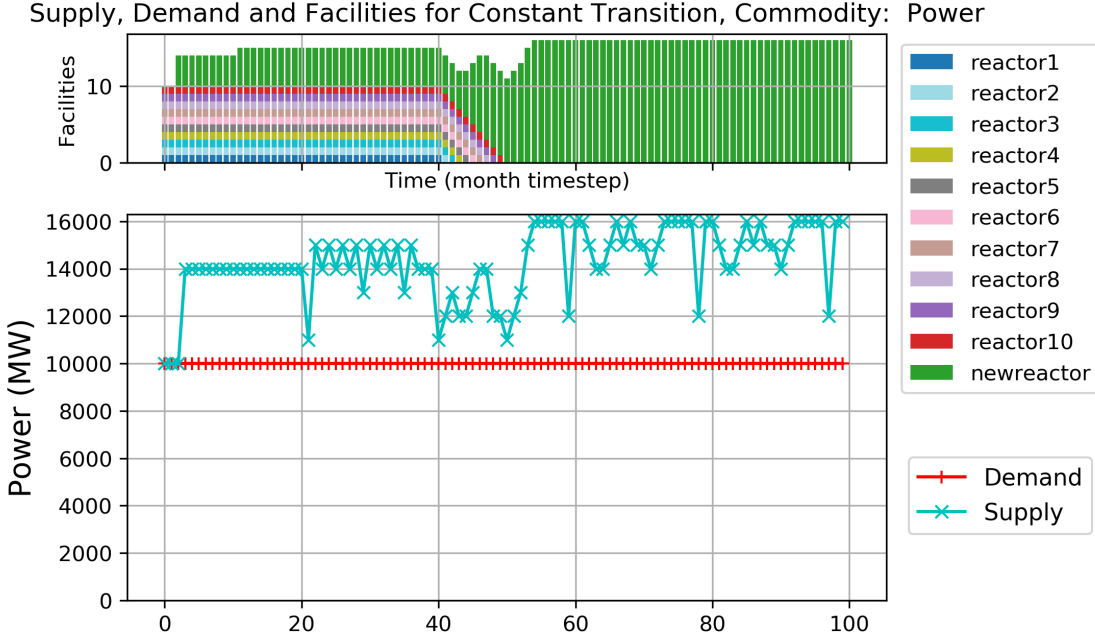


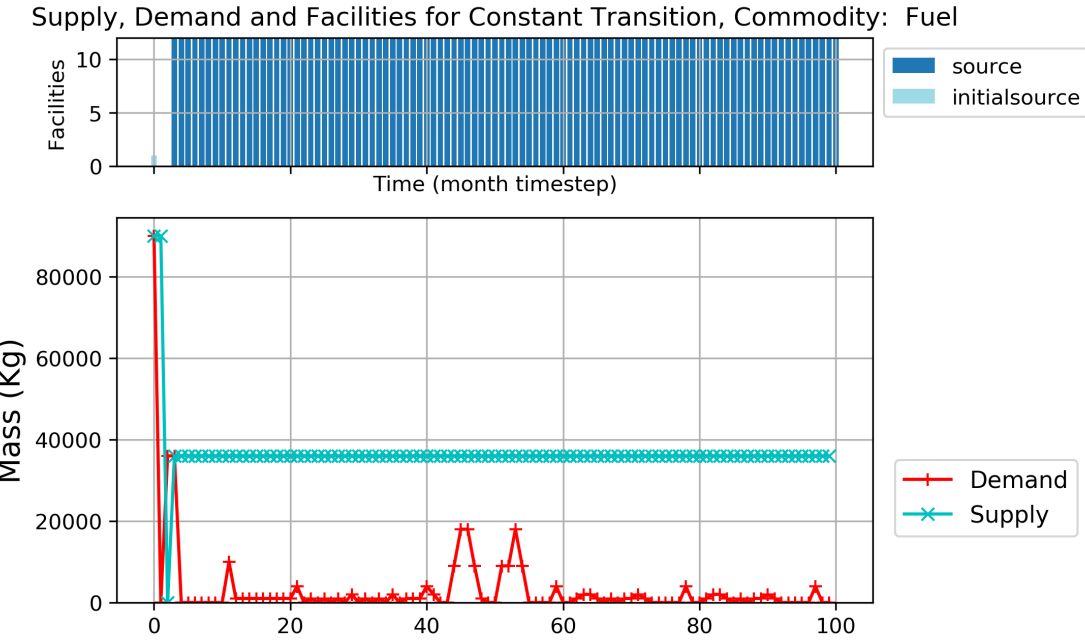
Figure 4.2: Power demand and supply, and reactor facility deployment for a simple constant power demand transition scenario with three facility types: `source`, `reactor`, and `sink`. There are no time steps with power undersupply [9].

of `d3ploy`. By using the FFT method for predicting demand and setting the power supply buffer to 3000MW (the capacity of 3 reactors), the user minimizes the number of undersupplied timesteps for every commodity.

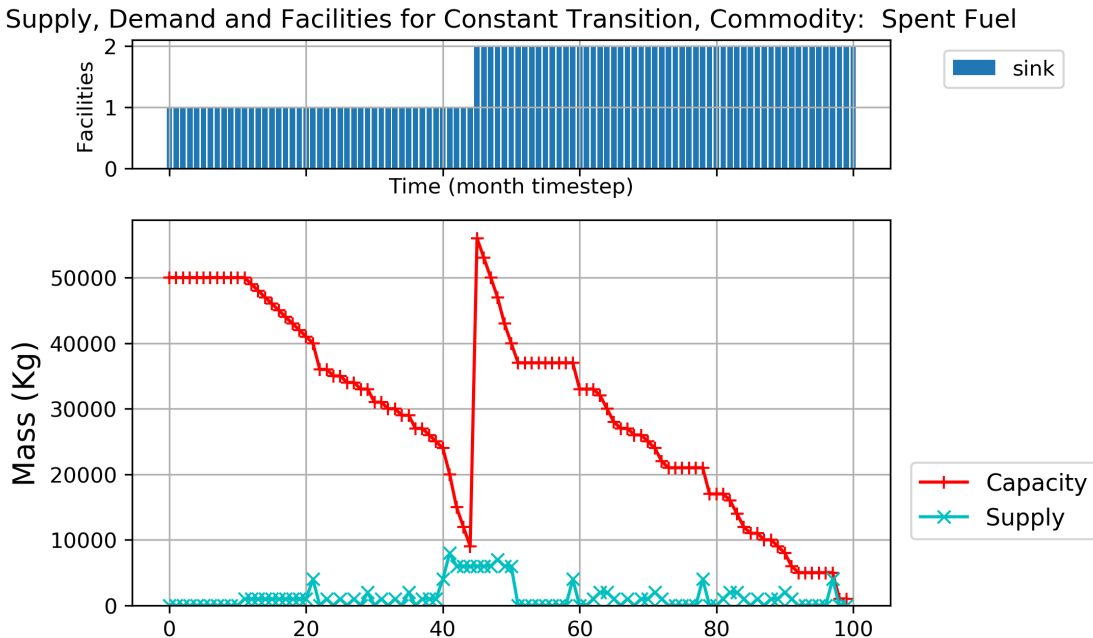
In Figure 4.3a, a large-throughput source facility is initially deployed to meet the large initial fuel demand for the commissioning of ten reactors. Deployment of a large-throughput source facility for the first few time steps ensures `d3ploy` does not deploy supporting facilities that become redundant at later times in the simulation. This reflects reality in which reactor manufacturers accumulate an appropriate amount of fuel inventory before starting up reactors.

#### 4.1.2 Simple Transition Scenario Simulation: Linearly Increasing Demand

Figures 4.4, 4.5a, and 4.5b demonstrate `d3ploy`'s capability to deploy reactors and supporting facilities to minimize undersupply when meeting linearly increasing power demand and subsequent secondary commodities demand. This transition utilizes a smaller power supply buffer compared with the constant power transition scenario. Table 4.2 shows the number of undersupplied timesteps. In Figure 4.4, there is no power supply gaps, demonstrating that `d3ploy` successfully deployed



(a) Fuel demand and supply, and source facility deployment. Reactor facilities demand fuel and source facilities supply it. There is only one time step with fuel undersupply [9].



(b) Spent fuel demand and supply, and sink facility deployment. Spent fuel is supplied by reactors and the capacity to store them is provided by sink facilities. There are no time steps with under-capacity of sink space [9].

Figure 4.3: Simple constant power demand transition scenario with three facility types: **source**, **reactor**, and **sink**.

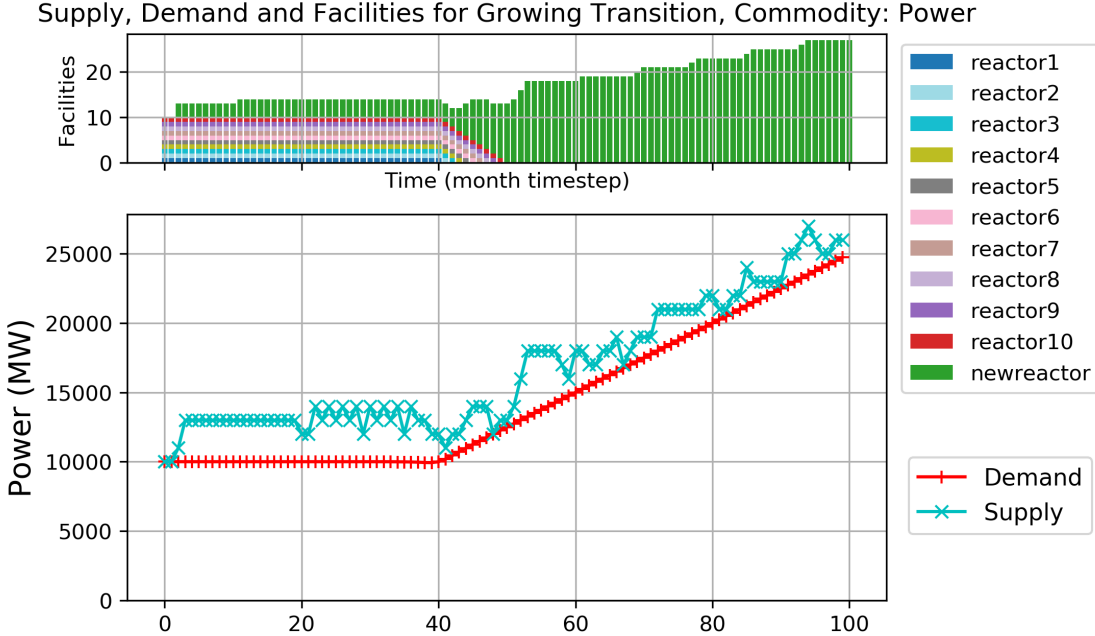


Figure 4.4: Power demand and supply, and reactor facility deployment plot for a simple linearly increasing power demand transition scenario with three facility types: `source`, `reactor`, and `sink`. There are no time steps with power undersupply[9].

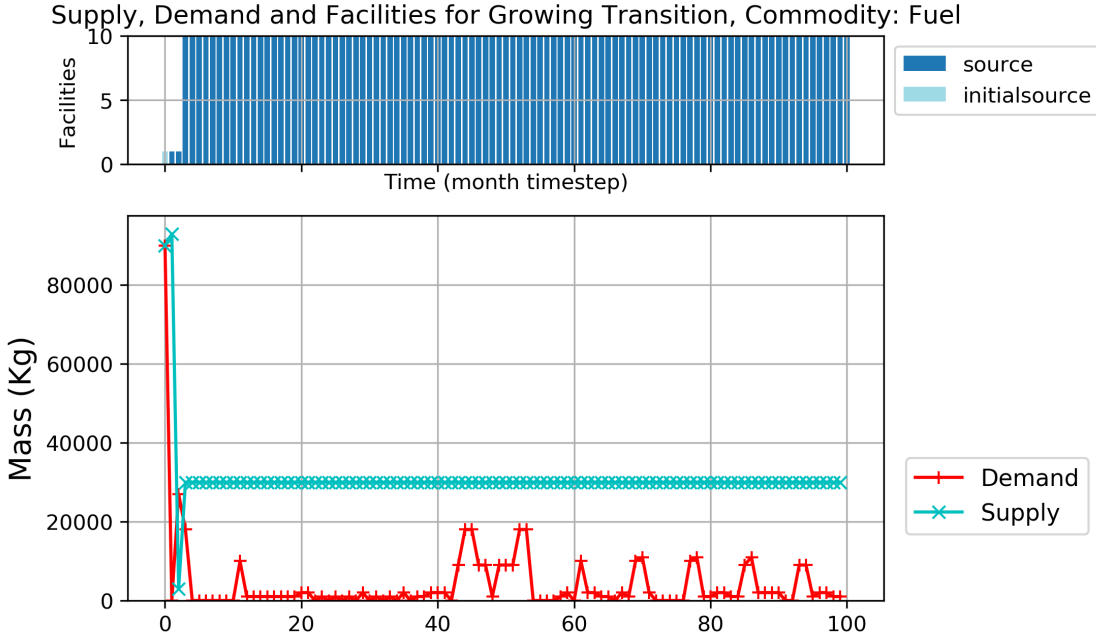
`source` `reactor`, and `sink` facilities to create the supply chain to meet the linearly-increasing power demand.

#### 4.1.3 Simple Transition Scenario Simulation: Sinusoidal Demand

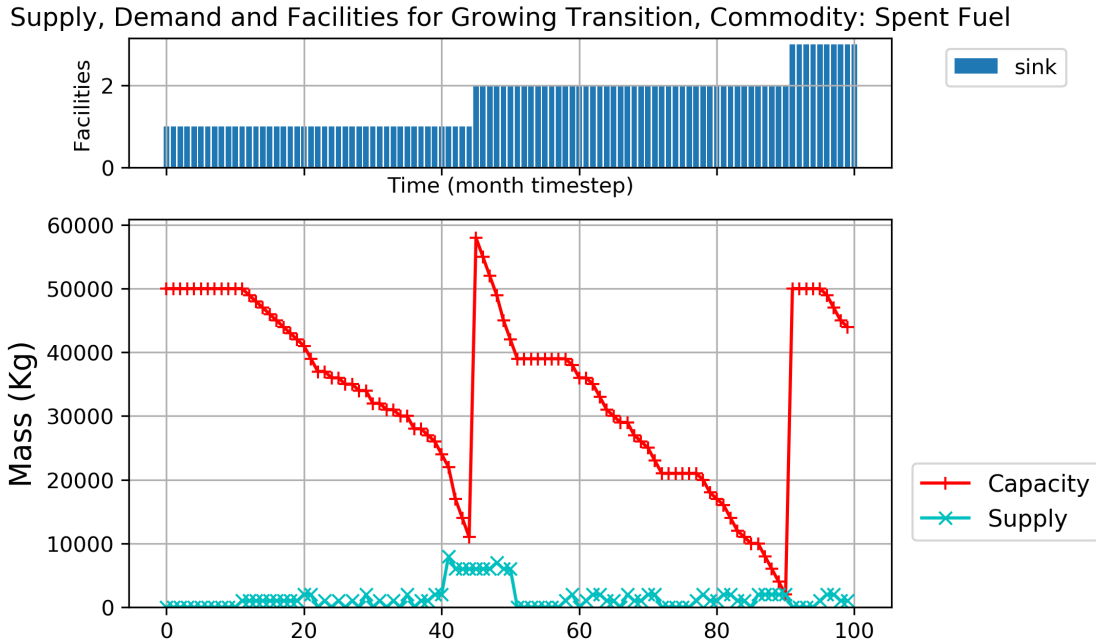
Real world power demand varies seasonally. Accordingly, a sinusoidal power demand with a period of 6 month best reflects reality. Figures 4.6, 4.7a, and 4.7b demonstrate `d3ploy`'s capability to deploy reactor and supporting facilities to meet a sinusoidal power demand. Table 4.2 shows the number of undersupplied timesteps. The `holt-winters` prediction method best minimizes power undersupply. This is because the `holt-winters` method excels in forecasting for repetitive seasonal time series data.

## 4.2 d3ploy Demonstration of EG01-30 Transition Scenario

In this section, we use `d3ploy` to set up the transition scenario from the current once through LWR fuel cycle (EG01) to a closed fuel cycle with continuous recycling of U/TRU in fast and thermal



(a) Fuel demand and supply, and source facility deployment plot. Reactor facilities demand fuel and source facilities supply it. There is only one time step with fuel undersupply [9].



(b) Spent fuel demand and supply, and sink facility deployment plot. Spent fuel is supplied by reactors and the capacity to store them is provided by sink facilities. There are no time steps with under-capacity of sink space [9].

Figure 4.5: Simple linearly increasing power demand transition scenario with three facility types: **source**, **reactor**, and **sink**.

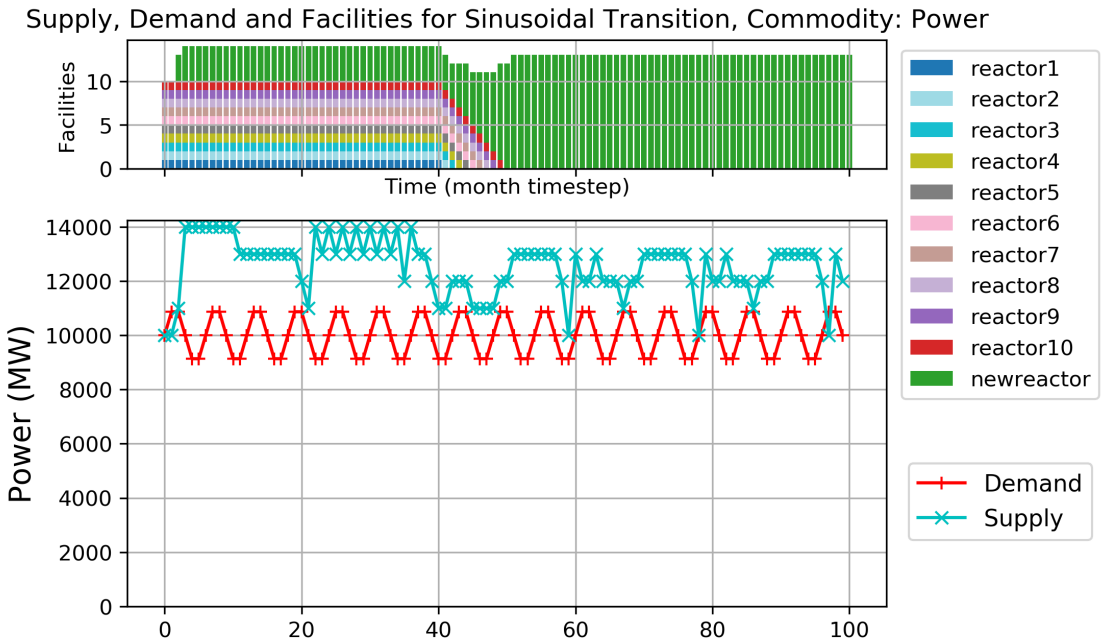
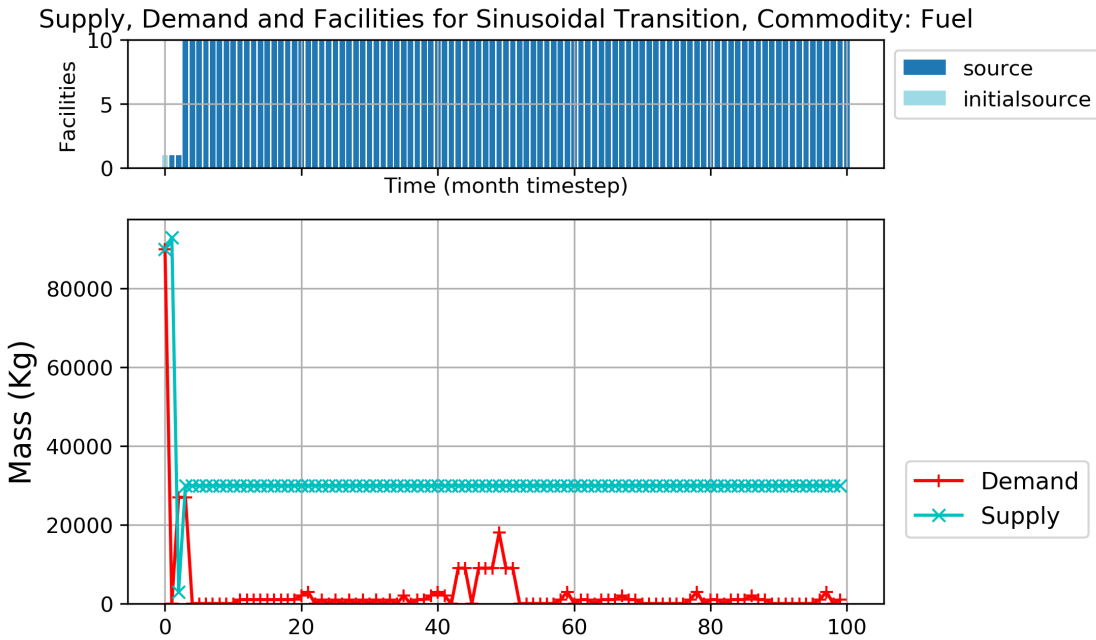


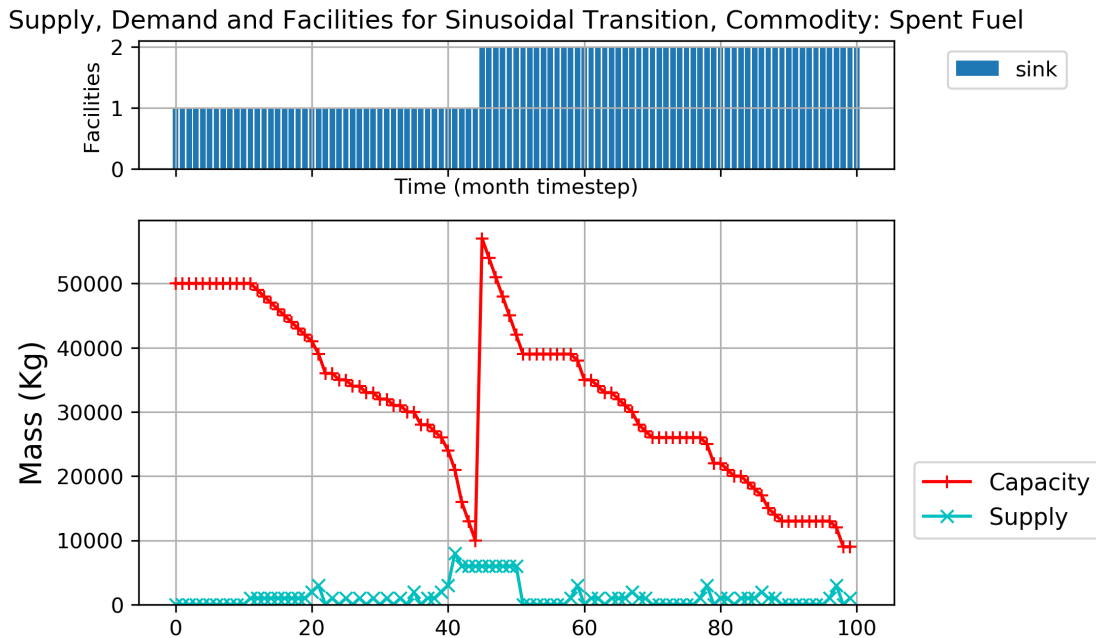
Figure 4.6: Power demand and supply, and reactor facility deployment plot for a simple sinusoidal power demand transition scenario with three facility types: `source`, `reactor`, and `sink`. There are no time steps with power undersupply [9].

Table 4.2: The total number of time steps with commodity undersupply for each simple transition scenario.

Simple Transition Scenario	Commodity	Undersupplied time steps [#]
<b>Constant Power</b>	Fuel	1
	Power	0
	Spent Fuel	0
<b>Linearly Increasing Power</b>	Fuel	1
	Power	0
	Spent Fuel	0
<b>Sinusoidal Power</b>	Fuel	1
	Power	1
	Spent Fuel	0



(a) Fuel demand and supply, and source facility deployment plot. Reactor facilities demand fuel and source facilities supply it. There is only one time step with fuel undersupply [9].



(b) Spent fuel demand and supply, and sink facility deployment plot. Spent fuel is supplied by reactors and the capacity to store them is provided by sink facilities. There are no time steps with under-capacity of sink space [9].

Figure 4.7: Simple sinusoidal power demand transition scenario with three facility types: **source**, **reactor**, and **sink**.

spectrum reactors (EG30). EG30 is one of the promising nuclear fuel cycles identified by DOE's evaluation and screening study (described in Section 2.2).

Figure 4.8 shows the setup of facilities and mass flows for EG01-30 in CYCLUS. In the EG01-30 transition scenario, the initial LWR fleet progressively decommissions at the 80-year mark, after which d3ploy deploys SFRs and MOX LWRs to meet a linearly increasing power demand. Transuranic elements from the spent fuel are recycled to produce MOX LWR and SFR fuel. The power demand equation:

$$P(t) = 60000 + \frac{250t}{12} \quad (4.1)$$

where:

$t$  = time step [month]

$P(t)$  = time-dependent power [MW]

We compared different prediction methods and power supply buffer sizes to determine the optimal d3ploy parameters for minimizing power undersupply in the EG01-30 CYCLUS transition scenario. The subsequent sections discuss the results from the comparison study.

#### 4.2.1 Comparison of Prediction Methods

We ran EG01-30 transition scenarios with different prediction methods to determine the prediction method that best minimizes power undersupply. In Figure 4.9, each histogram represents the number of time steps with undersupply or under capacity for all commodities for each prediction method. Table 4.3 shows the number of time steps with power undersupply for the linearly increasing power EG01-30 transition scenario. Figure 4.9 and Table 4.3 demonstrate that the FFT and POLY methods perform the best for the EG01-30 transition scenario, with the fewest time steps with power undersupply.

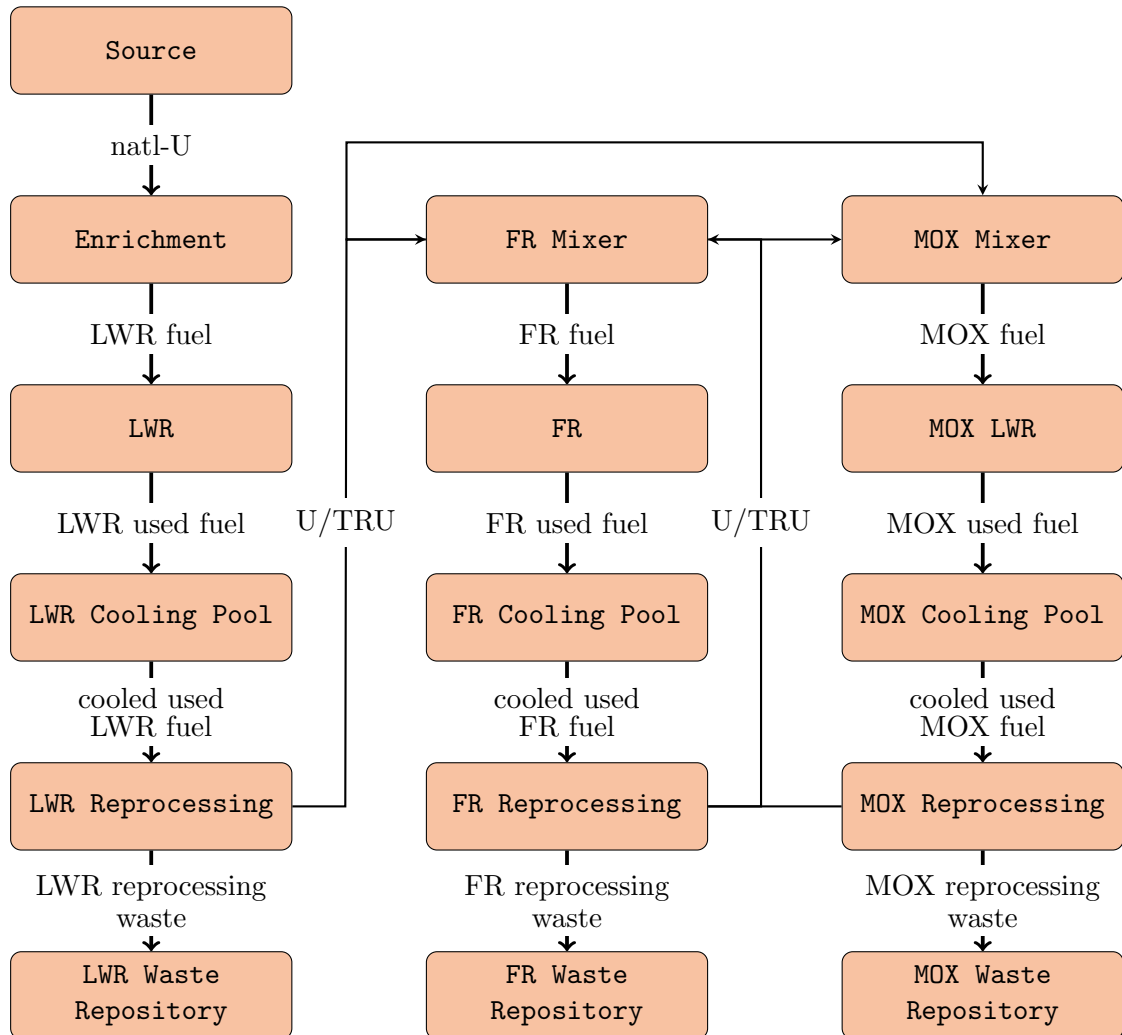


Figure 4.8: Facility and mass flow for the EG01-EG30 transition scenario. EG01 is the current once through LWR fuel cycle. EG30 is a closed fuel cycle with continuous recycling of U/TRU in fast and thermal reactors.

EG1-30: Time steps with an undersupply or under capacity of each commodity for different prediction methods

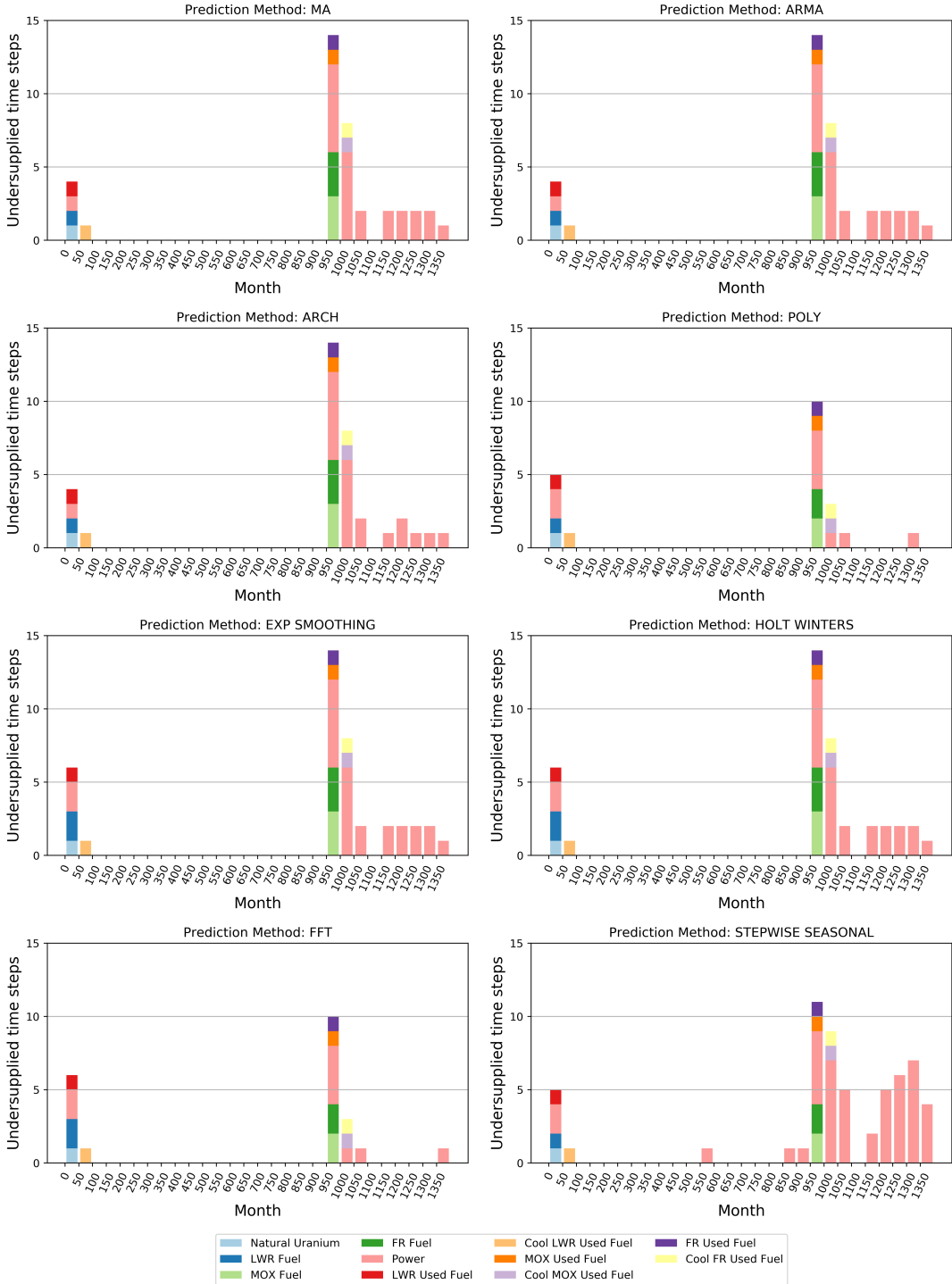


Table 4.3: Total number of time steps with power undersupply for the EG01-30 transition scenario for different prediction methods.

<b>Algorithm</b>	<b>EG01-30: No. of Time Steps with Power Undersupply</b>
MA	24
ARMA	24
ARCH	21
POLY	9
EXP-SMOOTHING	25
HOLT-WINTERS	25
FFT	9
SW-SEASONAL	51

#### 4.2.2 Comparison of Power Buffer Sizes

For the EG01-30 linearly increasing power demand transition scenario, the power buffer size is varied for both FFT and POLY methods. Varying the power buffer size does not impact the number of undersupplied time steps for the transition scenario with the POLY prediction method. For the transition scenario with FFT prediction method, Figure 4.10 and Table 4.4 show that with increased buffer size, the number of power undersupply time steps decreases. The cumulative undersupply is minimized with an 8000MW buffer. However, this means 8 extra reactors are required, which is unrealistic. In Figure 4.10, a 2000MW buffer size has 6 time steps with undersupply, while a 8000MW buffer size has 5 time steps with undersupply. The extra commissioning of 6 reactors does not justify the 1 time step. For a 2000MW buffer size simulation, undersupply time steps occur at the beginning of the simulation and for two time steps when the transition begins. This is expected since without time series data at the beginning of the simulation, `d3ploy` takes a few time steps to collect time series data about power demand to predict and start deploying reactor and supporting fuel cycle facilities. In reality, the power undersupply during the transition can be filled by coordinating refueling or short-term use of alternative energy sources. Therefore, a buffer of 2000MW minimizes the power undersupply for the EG01-EG30 transition scenario with the FFT prediction method.

### EG01-30: Power Undersupply vs. Power Buffer Size

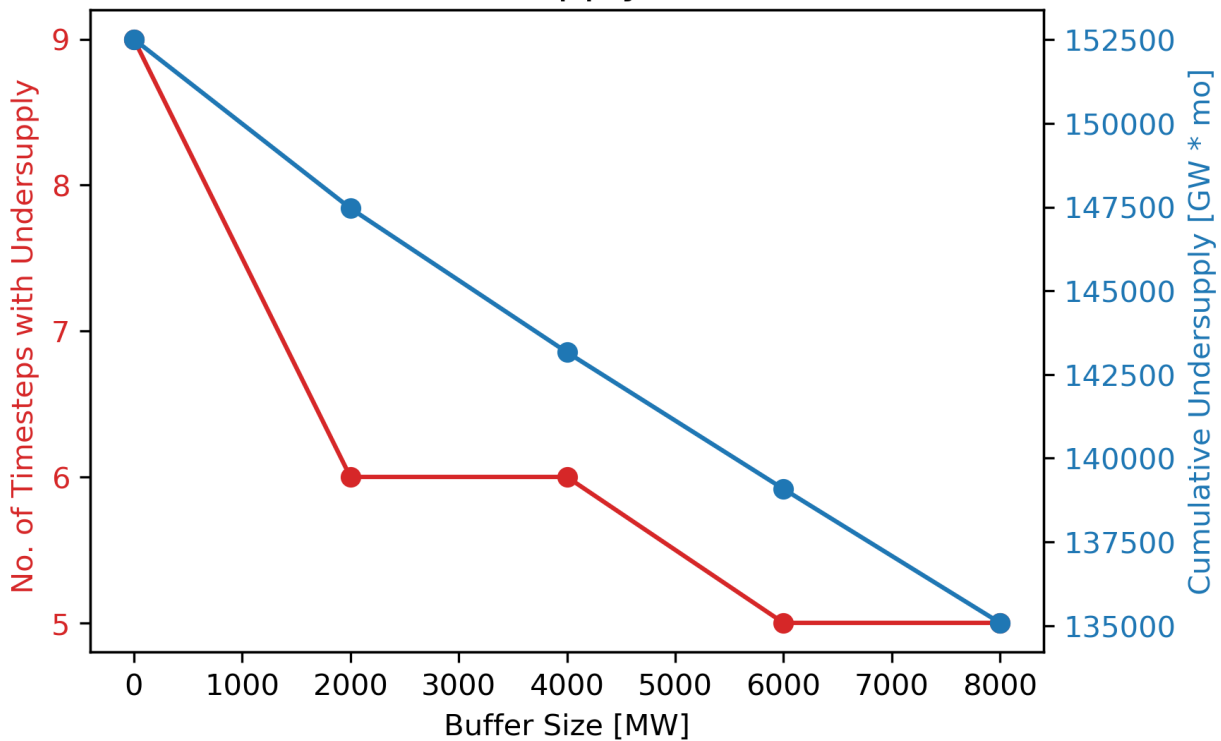


Figure 4.10: The effect of power buffer size on power undersupply for the EG01-30 transition scenario with linearly increasing power demand using the FFT method.

Table 4.4: Dependency of the power undersupply on the buffer size for EG01-EG30 transition scenarios with linearly increasing power demand using the FFT prediction method. There is less power undersupply for a larger power buffer size.

Buffer [MW]	Undersupply	EG01-30
<b>0</b>	Time steps [<#] ]	9
	Cumulative [ $GW \cdot mo$ ]	152517
<b>2000</b>	Undersupplied [<#] ]	6
	Cumulative [ $GW \cdot mo$ ]	147166
<b>4000</b>	Time steps [<#] ]	6
	Cumulative [ $GW \cdot mo$ ]	143166
<b>6000</b>	Time steps [<#] ]	5
	Cumulative [ $GW \cdot mo$ ]	139083
<b>8000</b>	Time steps [<#] ]	5
	Cumulative [ $GW \cdot mo$ ]	135083

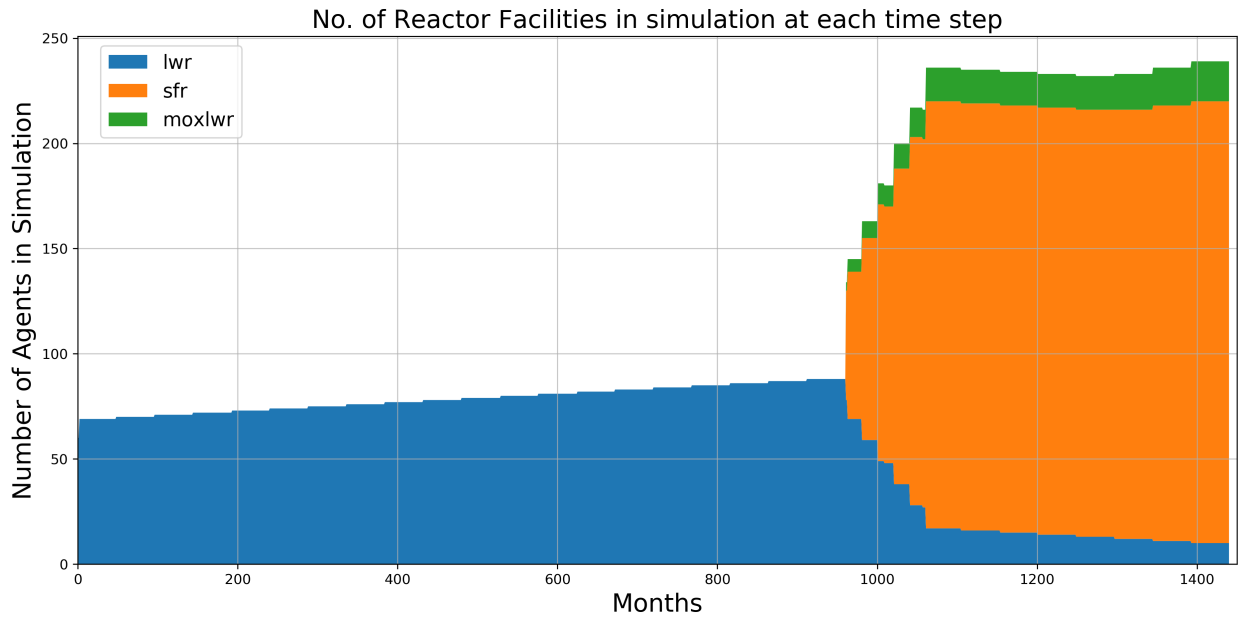
#### 4.2.3 Demonstration of Best Performance Model

Table 4.5 shows `d3ploy` input parameters for the EG01-EG30 transition scenario that minimize undersupply of power and minimize the undersupply and under capacity of the other commodities in the simulation. The need for commodity buffers reflects reality in that a supply buffer is usually maintained to ensure continuity in the event of an unexpected failure in the supply chain.

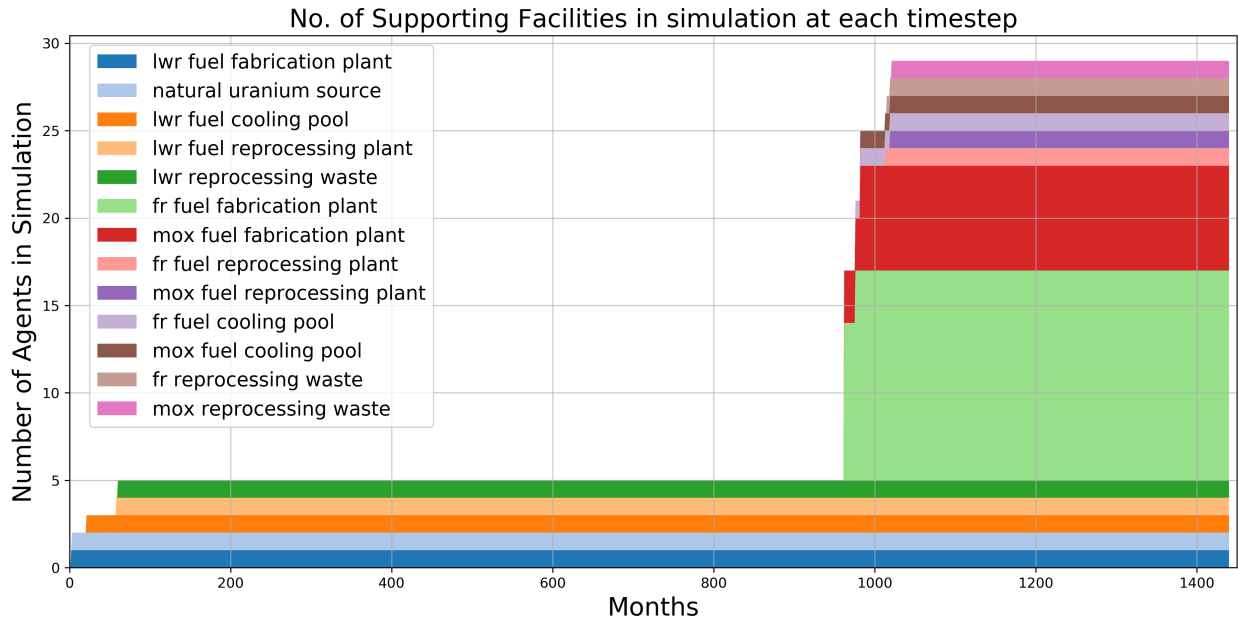
Figure 4.11 shows the time-dependent deployment of reactors and supporting facilities for the EG01-30 linearly increasing power demand transition scenario in which LWRs transition to MOX LWRs and SFRs.

### 4.3 Chapter Summary

In this chapter, we demonstrate `d3ploy`'s automatic deployment of fuel cycle facilities to meet constant, linearly increasing, and sinusoidal power demand in simple three-facility transition scenarios. Knowing that `d3ploy` works for simple transition scenarios, we use `d3ploy` to set up a complex transition from the current once through LWR fuel cycle (EG01) to a closed fuel cycle with continuous recycling of U/TRU in fast and thermal spectrum reactors (EG30). We demonstrate that



(a) EG01-30: Reactor Deployment



(b) EG01-30: Supporting Facility Deployment

Figure 4.11: Time dependent deployment of reactor and supporting facilities in the EG01-30 linearly increasing power demand transition scenario. d3ploy automatically deploys reactor and supporting facilities to setup a supply chain to meet linearly increasing power demand of  $60000 + 250t/12$  MW during a transition from LWRs to MOX LWRs and SFRs [9].

Table 4.5: `d3ploy`'s input parameters for the EG01-EG30 transition scenario which minimize undersupply for power and minimizes the undersupply and under capacity for other facilities.

d3ploy Input Parameter		EG01-30
<b>Required</b>	Demand driving commodity	Power
	Demand equation [MW]	$60000+250t/12$
	Prediction method	FFT
<b>Optional</b>	Deployment driving method	Installed Capacity
	Buffer type	Absolute
	Power buffer size [MW]	2000
	Transition start date [Month]	960 (Year 80)
Fleet share percentage [%]		MOX LWR: 15%, SFR: 85%

`d3ploy` can automatically deploy fuel cycle facilities to meet a linearly increasing power demand in the EG01-EG30 transition scenario. In the next chapter, `d3ploy` ensures automatic transition set up for sensitivity analysis studies of this EG01-30 transition scenario.

# Chapter 5

## Results: Sensitivity Analysis

In this chapter, we use DYMOND and CYCLUS to conduct sensitivity analysis studies of the EG01-30 nuclear fuel cycle transition scenario. We use Dakota-CYCLUS (`dcwrapper`) and Dakota-DYMOND coupling (`ddwrapper`) to perform one-at-a-time sensitivity analysis (SA), synergistic SA, and global SA. This chapter has six sections:

- **Transition Scenario Specifications.** We describe the EG01-EG30 transition scenario specifications used in the CYCLUS and DYMOND sensitivity analysis studies.
- **Sensitivity Analysis Evaluation Metrics.** We define evaluation metrics to determine the basis of comparison for sensitivity analysis of nuclear fuel cycle transition scenarios.
- **One-at-a-time sensitivity analysis.** We vary one input parameter at a time and evaluate its impact on the evaluation metrics.
- **Synergistic sensitivity analysis.** We vary two input parameters at a time and evaluate their impact on the evaluation metrics.
- **Global sensitivity analysis.** We vary all the input parameters to evaluate their global impact on the evaluation metrics.
- **Chapter Summary**

### 5.1 Transition Scenario Specification

Both DYMOND and CYCLUS sensitivity analyses use the EG01-30 transition scenario. We use a constant power demand of 430TWhe/y for the DYMOND simulation and a linearly increasing power demand of  $60000 + 250t/12MW$  for the CYCLUS simulation. The specifications for the

Table 5.1: OECD Benchmark Transition Scenario Specifications [34]

Input Parameter	Value
Demand driving commodity	Power
Demand equation [TWhe/y]	430
Transition Start Date [yr]	82
Fleet share ratio [%]	MOX LWR: 15 SFR: 85

supporting fuel cycle facilities are different for CYCLUS and DYMOND. This is because CYCLUS models supporting fuel cycle facilities as discrete agents, while DYMOND uses fleet-based modeling for all supporting fuel cycle facilities.

### 5.1.1 DYMOND

The specifications of the EG01-30 transition scenario used in the DYMOND sensitivity analysis are described in the DYMOND OECD benchmark transition scenario presented at the 17th Meeting of Expert Group on Advanced Fuel Cycle Scenarios in France in 2017 [34]. The OECD benchmark scenario is based on the EG01-30 transition scenario in which a PWR fleet is transitioned to a mixed fleet of MOX PWRs and SFRs. Table 5.1 describes those high-level OECD benchmark transition scenario specifications.

### 5.1.2 Cyclus

The CYCLUS transition scenario sensitivity analysis uses the linearly increasing power demand EG01-30 transition scenario (described in Section 4.2). Figure 4.8 shows the facility and mass flow for this transition scenario in CYCLUS. Tables 4.5 and 5.2 shows the input parameters for d3ploy and facilities in the transition scenario. The `reactor` facility used in the CYCLUS simulation is a recipe reactor; it accepts a fresh fuel recipe and outputs a spent fuel recipe. The recipes used for the LWR, MOX LWR, and SFR are based on recipes generated by VISION [9] that closely match EG30 scenario specifications in Appendix B of the Department of Energy (DOE) Evaluation and Screening Study (E&S study) [51].

Table 5.2: CYCLUS facility input parameters for EG01-EG30 transition scenario that minimizes undersupply of power and minimizes the undersupply and under capacity of other commodities.

<b>Facility</b>	<b>Input Parameter</b>	<b>Value</b>
<b>LWR</b>	Lifetime [months]	960
	Cycle time [months]	18
	Refuel time [months]	1
	Rated Power [MWe]	1000
<b>MOX LWR</b>	Lifetime [months]	960
	Cycle time [months]	18
	Refuel time [months]	1
	Rated Power [MWe]	1000
<b>SFR</b>	Lifetime [months]	720
	Cycle time [months]	12
	Refuel time [months]	1
	Rated Power [MWe]	333
<b>Cooling Pools</b>	Used fuel storage time [years]	3

## 5.2 Sensitivity Analysis: Evaluation Metrics

Evaluation metrics and their associated output variables must be defined to determine the basis of comparison for sensitivity analysis of nuclear fuel cycle transition scenarios. The E&S study [51] evaluated transition scenarios using nine metrics: nuclear waste management, proliferation risk, nuclear material security risk, safety, environmental impact, resource utilization, development and deployment risk, institutional issues, financial risk, and economics. These nine metrics are narrowed down into four categories: environmental impact, economics, proliferation risk and resource utilization [36].

Output indicators provide a single representative value to measure impact of the variation of an input parameter on a performance metric [1]. Three types of output indicators are introduced [1]: (1) the final value at the end of simulation (2) the maximum value during simulation, and (3) the cumulative sum over the whole simulation. A different output indicator is used depending on the nature of the output parameter. In addition, we include a separate proliferation-related indicator, quality of Plutonium, to be used for proliferation risk metrics:

$$\text{Quality of } Pu = \frac{Pu_{239} + Pu_{241}}{Pu_{238} + Pu_{240} + Pu_{242} + Pu_{243} + Pu_{244}} \quad (5.1)$$

The four evaluation metrics are:

- **Waste Management.** All nuclear fuel cycles require waste disposal capabilities and long-term isolation of some wastes [51]. We measure this metric based on the high level waste inventory and depleted uranium inventory.
- **Proliferation Risk.** Assessing proliferation risk is complex and challenging, with the dominant factor being facility location [51]. However, since we do not consider locations in this work, we measure proliferation risk based on plutonium inventory in cooling pools, high level waste, and reprocessing facilities.
- **Resource Utilization.** We measured resource utilization based on the amount of uranium ore used.
- **Goodness of Transition.** We introduced the goodness of transition metric to measure the success of a transition scenario simulation. A successful transition scenario minimizes total idle reactor capacity, and minimizes the length of the transition which is defined as the date of final idle capacity minus the transition start date.

Table 5.3 shows each evaluation metric's associated output variables and their indicators.

The operational conditions for the advanced reactors and the specifics of the transition scenario are variable since the fuel cycle simulator is modeling future trajectories. In the transition scenarios, we vary the following input parameters:

- **Length of used fuel cooling time.** By evaluating how length of used fuel cooling time impacts evaluation metrics, we can determine if online reprocessing (0 yr cooling time) is desirable compared to off-site reprocessing, and the logistics required to meet the ideal used fuel cooling time.
- **Fleet share ratio of MOX LWR and SFR reactors.** In the EG01-EG30 transition scenario, we transition from LWRs to MOX LWRs and SFRs. The MOX LWRs and SFRs

Table 5.3: Evaluation metrics and their associated output variables.

Evaluation Metrics	Output Variable	Indicators
<b>Waste Management</b>	High Level Waste Inventory	Final
	Depleted Uranium	Final
<b>Proliferation Risk</b>	Pu in Cooling Pools (CP)	Max, Quality
	Pu in HLW	Max, Quality
	Pu in Reprocessing Facilities (RPR)	Max, Quality
<b>Resource Utilization</b>	Uranium Ore Used	Sum
	Total Idle Capacity	Sum
<b>Goodness of Transition</b>	Date of Final Idle Capacity	Final
	Length of transition	-

have different reprocessing demands. We evaluate the impact of ratio of MOX LWRs and SFRs on the evaluation metrics.

- **Introduction date of advanced reactor technology (Transition Year).** Transition year is dependent on the technology-readiness of advanced reactor and reprocessing technologies. By evaluating how the transition year impacts the evaluation metrics, we inform on when advanced technologies must be ready.

In the following sections, we conduct one-at-a-time, synergistic, and global sensitivity analysis of these three input parameters and quantify the evaluation metric impact.

### 5.3 One-at-a-time Sensitivity Analysis

The one-at-a-time sensitivity analysis technique estimates the isolated effect of one input variable. This approach is useful as it gives each variable's local impact on the performance metrics.

#### 5.3.1 Length of cooling time for used fuel

In the DYMOND and CYCLUS EG01-30 transition scenarios, we varied used fuel cooling time from 0 to 8 years. We compared these simulations based on the evaluation metrics described in Table 5.3.

Table 5.4: DYMOND: Assessment of the impact of used fuel cooling time variation on evaluation metrics (waste management, resource utilization, and goodness of transition) for the OECD benchmark transition scenario [7].

Scenario	Environmental Impact		Resource Utilization	Goodness of Transition			
	Used Fuel Cooling Time [yr]	Final HLW [kg]	Final Depleted U [kg]	Resource Utilization	Total Idle Capacity [MW]	Final Idle Capacity Year	Length of Transition [yrs]
0	0	1103.2	916933.4	16188.8	30148.8	301	227
1	1	1101.6	916618.2	16188.8	30148.8	301	227
2	2	1105.7	916237.6	16188.8	30148.8	301	227
3	3	1108.3	916268.7	16188.8	256588.8	301	227
4	4	1099.8	916962.4	16188.8	1338604.8	301	227

## DYMOND

Tables 5.4 and 5.5 show the values of output variables associated with the environmental impact, resource utilization, and goodness of transition evaluation metrics for each scenario. Tables 5.6 and 5.7 show each scenario's percentage difference compared with the base case of 'Cooling Time = 2 years' scenario.

In Table 5.4, total idle capacity in the simulation increases for used fuel cooling time of 3 years onwards. This is because the fuel management strategy in the DYMOND OECD benchmark scenario was manually edited to work best with a 2 year used fuel cooling time. The idle capacity in cooling time of 3 years onwards could be avoided by manually changing the fuel management strategy in the DYMOND input file for the scenario. We did not manually change the fuel management strategy because this is a one-at-a-time sensitivity analysis study and, thus, only used fuel cooling time was varied.

In Table 5.7, compared with the base case, as cooling time increases, maximum Pu in the cooling pools increases. This is expected since cooling pools amass a larger inventory of used fuel when cooling time increases. The quality of Pu in the cooling pools also increases as cooling time increases. This is due to other isotopes decaying into Pu-239 and Pu-241 in the cooling pools.

## Cyclus

Tables 5.8 and 5.9 show the values of output variables associated with the environmental impact, resource utilization, and goodness of transition evaluation metrics for each scenario. Tables 5.10

Table 5.5: DYMOND: Assessment of the impact of used fuel cooling time variation on evaluation metrics (proliferation risk) for the OECD benchmark transition scenario [7].

Scenario Used Fuel Cooling Time [yr]	Proliferation Risk					
	Max Pu in CP [kg]	Quality at CP max Pu	Max Pu in HLW [kg]	Quality at HLW max	Max Pu in RPR [kg]	Quality at RPR max
	Pu	Pu	Pu	Pu	Pu	Pu
0	0.0	0	18.374	0.650	208.6	-
1	105.2	0.652	18.385	0.652	208.6	-
2	196.8	0.622	18.409	0.653	208.6	-
3	264.8	0.659	18.189	0.654	208.6	-
4	348.2	0.671	16.805	0.658	208.6	-

Table 5.6: DYMOND: Impact of variation in used fuel cooling times on evaluation metrics (waste management, resource utilization, and goodness of transition) for OECD benchmark transition scenario. The numbers in the table represent the percentage difference between an output variable from each scenario and the base case scenario (Cooling time = 2 years) [7].

Scenario Used Fuel Cooling Time [yr]	Environmental Impact		Resource Utilization Uranium Ore Used [%]]	Goodness of Transition		
	Final HLW [%]	Final Depleted U [%]		Total Idle Capacity [%]	Final Idle Capacity Year [%]	Length of Transition [%]
	0	0.076		0.0	0.000	0.0
1	-0.364	0.042		0.0	0.000	0.0
2						
3	0.234	0.003		0.0	751.075	0.0
4	-0.529	0.079		0.0	4339.994	0.0

- $sensitivity \leq 1\%$
- $1\% < sensitivity < 10\%$
- $sensitivity \geq 10\%$

Table 5.7: DYMOND: Impact of variation in used fuel cooling times on evaluation metrics (proliferation risk) for OECD benchmark transition scenario. The numbers in the table represent the percentage difference between an output variable from each scenario and the base case scenario (Cooling time = 2 years) [7].

Scenario Used Fuel Cooling Time [yr]	Proliferation Risk					
	Max Pu in CP [%]	Quality at CP max Pu	Max Pu in HLW [%]	Quality at HLW max	Max Pu in RPR [%]	Quality at RPR max
		[%]	Pu [%]		Pu [%]	
0	-100.0	-100.00	-0.19	-0.459	0.0	-
1	-46.5	4.82	-0.13	-0.153	0.0	-
2						
3	34.5	5.95	-1.20	0.153	0.0	-
4	76.9	7.88	-8.71	0.766	0.0	-

- *sensitivity*  $\leq 1\%$
- $1\% < \text{sensitivity} < 10\%$
- $\text{sensitivity} \geq 10\%$

and 5.11 show each scenario's percentage difference compared with the base case of 'Cooling Time = 2 years' scenario.

In Table 5.10, most evaluation metrics do not change with variation in the used fuel cooling time, except for the final HLW amount. Final HLW amount decreases for a longer used fuel cooling time. In Table 5.11, compared with the base case, as cooling time increases, maximum Pu in the cooling pools increases. This is similar to the result for the DYMOND transition scenario (Table 5.7). This is expected since there will be a larger inventory of used fuel in the cooling pools when cooling time increases. Maximum Pu in HLW and reprocessing facilities, and their corresponding Pu quality, decrease for a longer cooling time. Variation in used fuel cooling time does not impact the resource utilization and goodness of transition evaluation metrics, slightly impacts the environmental impact evaluation metric, and severely impacts the proliferation risk evaluation metric. A longer used fuel cooling time means that more Plutonium is collected in a single facility.

### 5.3.2 Fleet share ratio of PWR MOX and SFR reactors

The fleet share ratio of MOX PWRs and SFRs was varied from 0:100 to 20:80 for the CYCLUS EG01-30 transition scenario. We compared these simulations based on the evaluation metrics described in Table 5.3.

Tables 5.12 and 5.13 show the values of output variables associated with the environmental

Table 5.8: CYCLUS: Assessment of the impact of used fuel cooling time variation on evaluation metrics (waste management, resource utilization, and goodness of transition) for EG01-EG30 transition scenario [10].

Scenario	Environmental Impact		Resource Utilization	Goodness of Transition		
	Final HLW [kg]	Final Depleted U [kg]		Total Idle Capacity [MW]	Final Idle Capacity Year	Length of Transition [yrs]
Used Fuel Cooling Time [yr]		Uranium Ore Used [kg]				
0	1.32e7	7.99e8	1.437e11	135.1	962	2
2	1.32e7	7.99e8	1.437e11	135.1	962	2
4	1.29e7	7.99e8	1.437e11	135.1	962	2
6	1.27e7	7.99e8	1.437e11	135.1	962	2
8	1.27e7	7.99e8	1.437e11	135.1	962	2

Table 5.9: CYCLUS: Assessment of the impact of used fuel cooling time variation on evaluation metrics (proliferation risk) for EG01-EG30 transition scenario [10].

Scenario	Proliferation Risk					
	Used Fuel Cooling Time [yr]	Max Pu in CP [kg]	Quality at CP max Pu	Max Pu in HLW [kg]	Quality at HLW max Pu	Max Pu in RPR [kg]
0	4.90e4	0.66	4.44e4	0.62	2.80e6	0.49
2	1.99e5	0.6	4.36e4	0.62	2.63e6	0.48
4	3.68e5	0.58	4.28e4	0.62	2.46e6	0.48
6	5.54e5	0.57	4.26e4	0.62	2.29e6	0.47
8	7.33e5	0.56	4.28e4	0.62	2.11e6	0.47

Table 5.10: CYCLUS: Impact of variation in used fuel cooling times on evaluation metrics (environmental impact, resource utilization, and goodness of transition) for EG01-EG30 transition scenario. The numbers in the table represent the percentage difference between an output variable from each scenario and the base case scenario (Cooling time = 2 years) [10].

Scenario	Environmental Impact		Resource Utilization	Goodness of Transition			
	Used Fuel Cooling Time [yr]	Final HLW [%]	Final Depleted U [%]	Uranium Ore Used [%]	Total Idle Capacity [%]	Final Idle Capacity Year [%]	Length of Transition [%]
0	1.15	0.0	0.0	0.0	0.0	0.0	0.0
2							
4	-1.28	0.0	0.0	0.0	0.0	0.0	0.0
6	-2.12	0.0	0.0	0.0	0.0	0.0	0.0
8	-2.65	0.0	0.0	0.0	0.0	0.0	0.0

- $sensitivity \leq 1\%$
- $1\% < sensitivity < 10\%$
- $sensitivity \geq 10\%$

Table 5.11: CYCLUS: Impact of variation in used fuel cooling times on evaluation metrics (proliferation risk) for EG01-EG30 transition scenario. The numbers in the table represent the percentage difference between an output variable from each scenario and the base case scenario (Cooling time = 2 years) [10].

Scenario Used Fuel Cooling Time [yr]	Proliferation Risk					
	Max Pu in CP [%]	Quality at CP max Pu	Max Pu in HLW [%]	Quality at HLW max	Max Pu in RPR [%]	Quality at RPR max
		[%]	Pu [%]		Pu [%]	
0	-75.39	8.99	1.83	0.08	6.2	1.45
2						
4	85.09	-3.34	-1.8	-0.12	-6.7	-1.06
6	178.5	-5.55	-2.25	-0.15	-13.13	-2.11
8	268.52	-7.23	-1.77	-0.22	-19.92	-3.0

- $sensitivity \leq 1\%$
- $1\% < sensitivity < 10\%$
- $sensitivity \geq 10\%$

impact, resource utilization, and goodness of transition evaluation metrics for each scenario. Tables 5.14 and 5.15 show each scenario's percentage difference compared with the base case of 'Fleet share = 15% MOX PWRs' scenario.

In Table 5.14, most evaluation metrics do not change for variation in fleet share ratio, except for the final amount of HLW in the scenario. The final amount of HLW is largest for 0% fleet share of MOX PWRs and decreases as the fleet share of MOX PWRs increases. In Table 5.15, maximum Pu in cooling pools and reprocessing facility increases for increasing fleet share ratio of MOX PWRs; however, the quality of Pu decreases. Maximum Pu in HLW decreases for a decreasing fleet share ratio of MOX PWRs, while the quality of Pu increases slightly. Variation in used fuel cooling time does not impact the resource utilization and goodness of transition evaluation metrics, slightly impacts the environmental impact evaluation metric, and severely impacts the proliferation risk evaluation metric. Therefore, if minimizing proliferation risk is a high priority, a transition scenario with a smaller fleet share of MOX PWRs is recommended to minimize the Pu amount in the cooling pools and reprocessing facilities.

### 5.3.3 Introduction year of advanced reactor technology

The introduction year of advanced reactor technology was varied from year 80 to 84 for the CYCLUS EG01-30 transition scenario. We compared these simulations based on the evaluation metrics

Table 5.12: CYCLUS: Assessment of the impact of variation in fleet share ratio of LWR MOX and SFR reactors on evaluation metrics (environmental impact, resource utilization, and goodness of transition) for EG01-30 transition scenario [10].

Scenario	Environmental Impact		Resource Utilization	Goodness of Transition		
	Final HLW [kg]	Final Depleted U [kg]		Total Idle Capacity [MW]	Final Idle Capacity Year	Length of Transition [yrs]
0	1.315e7	7.988e8	1.437e11	135.1	962	2
5	1.305e7	7.988e8	1.437e11	135.1	962	2
10	1.305e7	7.988e8	1.437e11	135.1	962	2
15	1.295e7	7.988e8	1.437e11	135.1	962	2
20	1.300e7	7.988e8	1.437e11	135.1	962	2

Table 5.13: CYCLUS: Assessment of the impact of variation in fleet share ratio of LWR MOX and SFR reactors on evaluation metrics (proliferation risk) for EG01-30 transition scenario [10].

Scenario	Proliferation Risk					
	Max Pu in CP [kg]	Quality at CP max Pu	Max Pu in HLW [kg]	Quality at HLW max Pu	Max Pu in RPR [kg]	Quality at RPR max Pu
0	2.56e5	0.66	45816.02	0.62	2357604.01	0.55
5	2.73e5	0.62	44338.72	0.62	2461421.31	0.51
10	2.79e5	0.61	44055.54	0.62	2513133.76	0.5
15	2.85e5	0.59	42905.59	0.62	2552142.82	0.48
20	2.91e5	0.58	43133.61	0.62	2605589.02	0.47

Table 5.14: CYCLUS: Impact of variation in fleet share ratio of LWR MOX and SFR reactors on evaluation metrics (environmental impact, resource utilization, and goodness of transition) for EG01-EG30 transition scenario. The numbers in the table represent the percentage difference between an output variable from each scenario and the base case scenario (PWR MOX fleet share = 15%) [10].

Scenario	Environmental Impact		Resource Utilization	Goodness of Transition		
	Final HLW [%]	Final Depleted U [%]		Total Idle Capacity [%]]	Final Idle Capacity Year [%]	Length of Transition [%]
0	1.49	0.0	0.0	0.0	0.0	0.0
5	0.75	0.0	0.0	0.0	0.0	0.0
10	0.71	0.0	0.0	0.0	0.0	0.0
15						
20	0.33	0.0	0.0	0.0	0.0	0.0

- $sensitivity \leq 1\%$
- $1\% < sensitivity < 10\%$
- $sensitivity \geq 10\%$

Table 5.15: CYCLUS: Impact of variation in fleet share ratio of LWR MOX and SFR reactors on evaluation metrics (proliferation risk) for EG01-EG30 transition scenario. The numbers in the table represent the percentage difference between an output variable from each scenario and the base case scenario (PWR MOX fleet share = 15%) [10].

Scenario MOX Fleet Share [%]	Proliferation Risk					
	Max Pu in CP [%]	Quality at CP max Pu	Max Pu in HLW [%]	Quality at HLW max	Max Pu in RPR [%]	Quality at RPR max
			[%]	Pu [%]		Pu [%]
0	-10.15	10.63	6.78	-0.48	-7.62	14.05
5	-4.22	4.34	3.34	-0.21	-3.55	6.57
10	-2.13	2.15	2.68	-0.09	-1.53	3.35
15						
20	2.1	-2.02	0.53	0.13	2.09	-2.9

- $sensitivity \leq 1\%$
- $1\% < sensitivity < 10\%$
- $sensitivity \geq 10\%$

described in Table 5.3.

Tables 5.16 and 5.17 show the values of output variables associated with the environmental impact, resource utilization, and goodness of transition evaluation metrics for each scenario. Tables 5.18 and 5.19 show each scenario's percentage difference compared with the base case of 'Transition Year = 80' scenario.

In Table 5.18, total idle capacity in the simulation is minimized at an advanced reactor introduction year of 80 onwards. Final HLW and depleted uranium increases for a later advanced reactor introduction year. In Table 5.19, maximum Pu in cooling pools has a mostly constant trend after advanced reactor introduction year of 80. For a later advanced reactor introduction year, maximum Pu in HLW increases, while maximum Pu in reprocessing facilities decreases; the quality of Pu is constant. Variation in used fuel cooling time does not impact the resource utilization evaluation metric, slightly impacts the environmental impact and proliferation risk evaluation metric, and severely impacts the goodness of transition evaluation metric. A later advanced reactor introduction year should be selected to ensure minimal idle reactor capacity.

Table 5.16: CYCLUS: Assessment of impact of variation in advanced reactor introduction year on evaluation metrics (environmental impact, resource utilization, and goodness of transition) for EG01-30 transition scenario [10].

Scenario	Environmental Impact		Resource Utilization	Goodness of Transition		
	Final HLW [kg]	Final Depleted U [kg]		Uranium Ore Used [kg]	Total Idle Capacity [MW]	Final Idle Capacity Year
80	1.295e7	7.988e8	1.437e11		135.1	962
81	1.306e7	7.988e8	1.437e11		120.9	972
82	1.322e7	8.033e8	1.437e11		121.1	980
83	1.336e7	8.078e8	1.437e11		121.1	980
84	1.333e7	8.078e8	1.437e11		121.1	980

Table 5.17: CYCLUS: Assessment of impact of variation in advanced reactor introduction year on evaluation metrics (proliferation risk) for EG01-30 transition scenario [10].

Scenario	Proliferation Risk					
	Max Pu in CP [kg]	Quality at CP max Pu	Max Pu in HLW [kg]	Quality at HLW max Pu	Max Pu in RPR [kg]	Quality at RPR max Pu
80	2.857e5	0.59	4.29e4	0.62	2.55e6	0.48
81	2.696e5	0.60	4.42e4	0.62	2.53e6	0.48
82	2.733e5	0.60	4.56e4	0.62	2.48e6	0.48
83	2.733e5	0.59	4.68e4	0.62	2.47e6	0.48
84	2.694e5	0.60	4.67e4	0.62	2.45e6	0.48

Table 5.18: CYCLUS: Impact of variation in advanced reactor introduction year on evaluation metrics (environmental impact, resource utilization, and goodness of transition) for EG01-EG30 transition scenario. The numbers in the table represent the percentage difference between an output variable from each scenario and the base case scenario (transition year = 80) [10].

Scenario	Environmental Impact		Resource Utilization	Goodness of Transition		
	Final HLW [%]	Final Depleted U [%]		Total Idle Capacity [%]	Final Idle Capacity Year [%]	Length of Transition [%]
80						
81	0.85	0.0	0.0	-10.51	1.04	-100.0
82	2.01	0.57	0.0	-10.36	1.87	-100.0
83	3.09	1.13	0.0	-10.36	1.87	-100.0
84	2.91	1.13	0.0	-10.36	1.87	-100.0

- $sensitivity \leq 1\%$
- $1\% < sensitivity < 10\%$
- $sensitivity \geq 10\%$

Table 5.19: CYCLUS: Impact of variation in advanced reactor introduction year on evaluation metrics (proliferation risk) for EG01-EG30 transition scenario. The numbers in the table represent the percentage difference between an output variable from each scenario and the base case scenario (transition year = 80) [10].

Scenario Transition Year	Proliferation Risk						
	Max Pu in CP [%]	Quality at CP max Pu	Max Pu in HLW [%]	Quality at HLW max	Max Pu in RPR [%]	Quality at RPR max	
		[%]	Pu [%]		Pu [%]		
80							
81	-5.64	0.67	3.23	-0.09	-0.86	0.02	
82	-4.37	1.15	6.45	-0.15	-2.44	0.09	
83	-4.37	0.07	9.19	-0.21	-2.99	-0.04	
84	-5.73	0.98	8.88	-0.25	-3.77	0.07	

- $sensitivity \leq 1\%$
- $1\% < sensitivity < 10\%$
- $sensitivity \geq 10\%$

## 5.4 Synergistic Sensitivity Analysis

Basic sensitivity analysis focuses on changing each input parameter one-at-a-time to see the effect on the output variables. However, this approach does not fully explore the input space as it does not consider the synergistic effects of the simultaneous variation of the input variables. In this section, we explore the effect of synergistic sensitivity analysis on the evaluation metrics. We explained synergistic analysis in Section 2.3.2.

### 5.4.1 Fleet Share Ratio and Introduction date of advanced reactor technology

The fleet share ratio between PWR MOX and SFR reactors and the introduction date of advanced reactor technology were synergistically varied for the EG01-30 transition scenario.

#### DYMOND

We evaluated 9 scenarios for a combination of fleet share ratio of 2%, 5%, 8% PWR MOX, and transition start date of year 82,83, and 84. We compared these simulations based on the evaluation metrics described in Table 5.3. Tables with the results of each scenario's performance for each evaluation metric are available in `ddwrapper` github repository [7].

Figures 5.1a, 5.1b, and 5.1c visualize the maximum amount of Pu in the spent fuel cooling,

primary feed, and high level waste (HLW) in storage inventories for varying fleet share and transition start year values. Pu in the spent fuel cooling inventory is minimized for PWR MOX fleet share ratio of 2% for all transition years and PWR MOX fleet share ratio of 8% for transition start year of 82 and 83. Pu in the primary feed inventory is minimized for PWR MOX fleet share ratio of 5% for all transition years and PWR MOX fleet share ratio of 8% for transition start year of 83 and 84. Pu in HLW in storage inventory is minimized for PWR MOX fleet share ratio of 2% for all transition years.

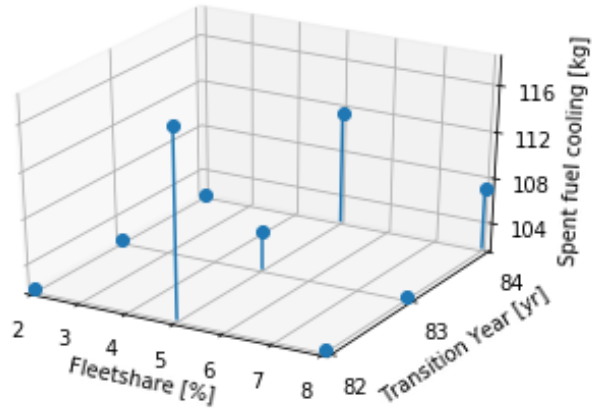
Figures 5.1a, 5.1b, and 5.1c communicate how fleet share ratio and introduction date of advanced reactor technology synergistically impact maximum Pu in various inventories in the nuclear fuel cycle. Similar synergistic studies can be conducted for the output variables in all the evaluation metrics to better utilize this information for decision making. The results from each study can be normalized, weighted, and combined to create an optimization surface similar to Figure 2.3 to determine the ideal fleet share ratio and transition year combination.

## Cyclus

We evaluated 25 scenarios for a combination of PWR MOX to SFR fleet share ratio of 0:100, 5:95, 10:90, 15:85, 20:80 and advanced reactor introduction date of year 80 to 84. Figures 5.2, 5.3, and 5.4 visualize the final amount of HLW, the final amount of depleted uranium, and the total amount of idle capacity in the scenario for varying fleet share and advanced reactor introduction date values.

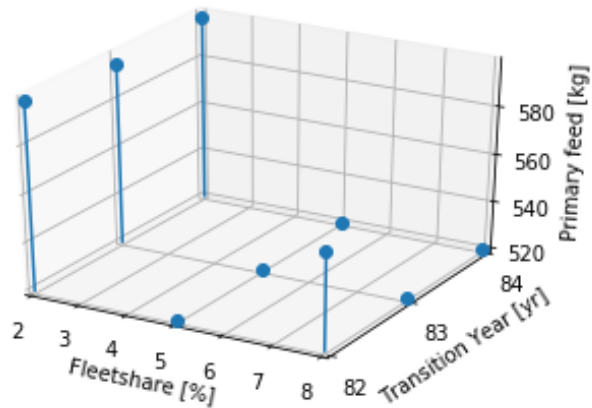
Figure 5.2 shows that for scenarios in which there is a smaller fleet share of MOX LWRs, and the transition begins later in the simulation, less high level waste is produced. For a later transition year, we assume the initial LWRs have a longer lifetime and thus, advanced reactors exist in the simulation for a shorter amount of time, resulting in a smaller production of reprocessing HLW waste. Also, MOX LWRs produce more HLW than SFRs. Figure 5.3 shows that as the introduction date of advanced reactors is pushed back, more depleted uranium is produced. This is due to the extended lifetime of the LWRs that utilize enriched natural uranium fuel that generates depleted uranium. Figure 5.4 shows that idle capacity is minimized for a later advanced reactor introduction date. Having a later introduction date of advanced reactor technology ensures a sufficiently large

3D plot of Spent fuel cooling



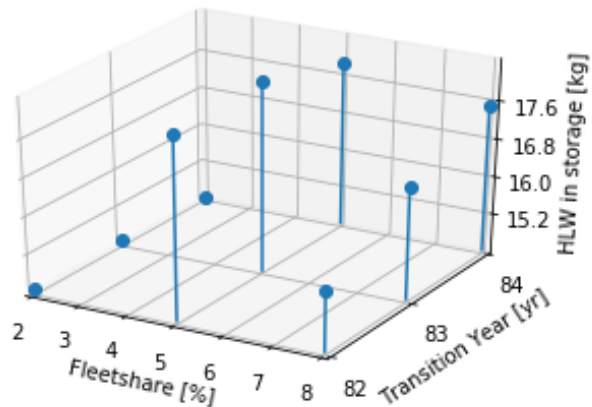
(a) Inventory: Spent fuel cooling

3D plot of Primary feed



(b) Inventory: Primary feed

3D plot of HLW in storage



(c) Inventory: HLW in storage

Figure 5.1: DYMOND EG01-30 Transition Scenario: Maximum amount of Pu [kg] in each inventory for varying fleet share and transition start date simulations [7].

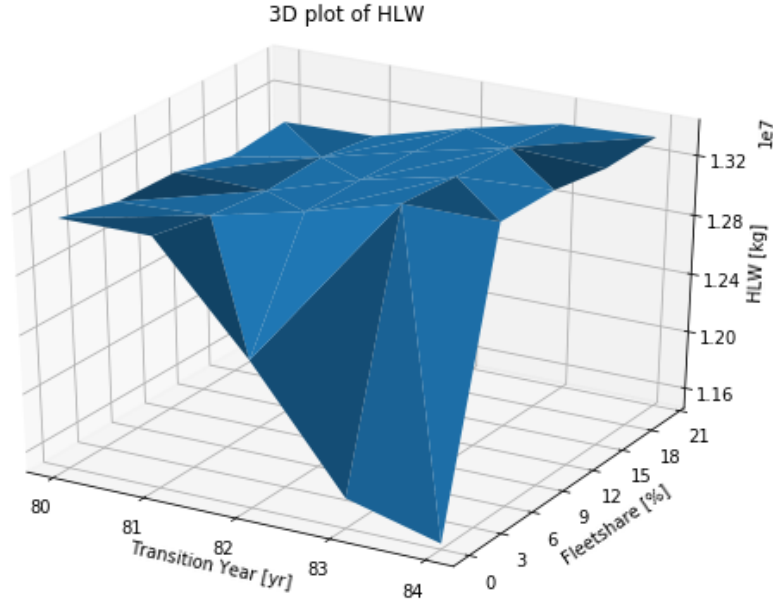


Figure 5.2: Impact on final amount of HLW [kg] when fleet share and transition start date are varied for the CYCLUS EG01-30 transition scenario [10].

inventory of transuranic elements is amassed to produce fuel for the MOX PWRs and SFRs. This avoids gaps in the supply chain that would otherwise result in idle advanced reactor capacity.

## 5.5 Global Sensitivity Analysis

We used `dcwrapper` to conduct a global sensitivity analysis study to generate Sobol indices, which tell us which input parameters have the most influence on each output variable. Section 2.3.3 describes this type of sensitivity analysis. It provides a more holistic view of the system than one-at-a-time (section 5.3) and synergistic (section 5.4) sensitivity analysis because it decomposes the variance of the output of the scenario simulation into fractions which are attributed to each input, giving a better idea of the most impactful input parameters. We could vary more than two variables in a synergistic sensitivity analysis, but it is difficult to visualize the results.

The input variables varied are fleet share ratio, transition start year, and used fuel cooling time. The output variables considered are the final amount of HLW, the final amount of depleted uranium, and total idle capacity. Table 5.20 provides the Sobol indices which is a summary of

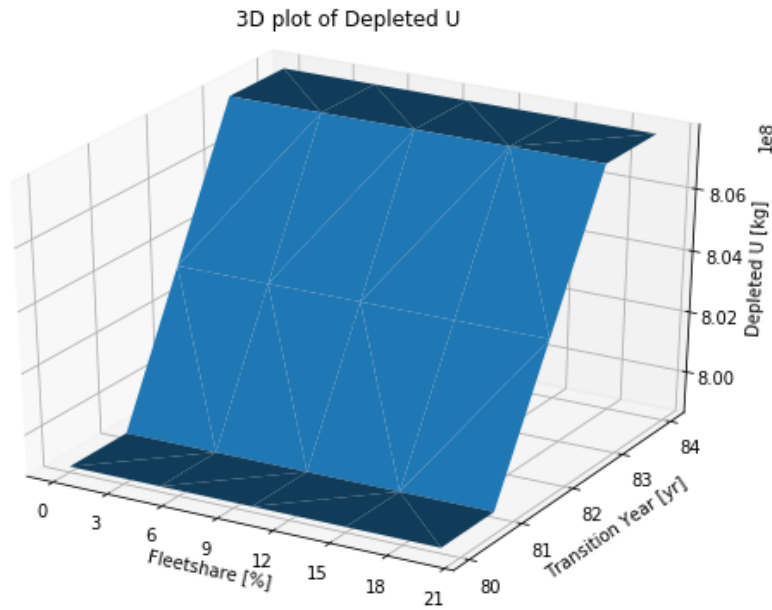


Figure 5.3: Impact on final amount of Depleted Uranium [kg] when fleet share and transition start date are varied for the CYCLUS EG01-30 transition scenario [10].

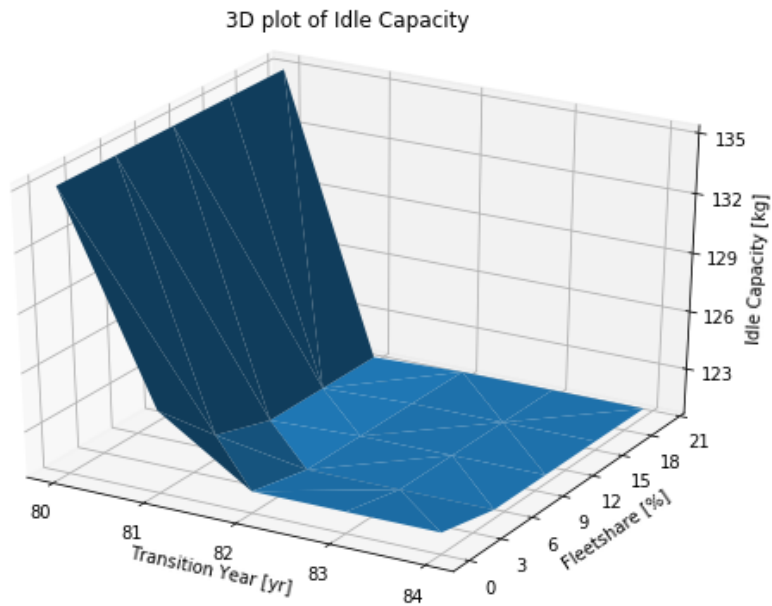


Figure 5.4: Impact on total amount of idle reactor capacity [MW] when fleet share and transition start date are varied for the CYCLUS EG01-30 transition scenario [10].

Table 5.20: The first order Sobol Indices for a global sensitivity analysis study of the impact of fleet share % of PWR MOX reactors, transition start year and used fuel cooling time on various output variables: final amount of HLW, final amount of depleted uranium, and total idle capacity in the simulation. The Sobol Indices are only comparable within each column, not within each row [10].

Input Variables	Performance Metrics		
	Final HLW	Final Depleted Uranium	Total Idle Capacity
Fleet Share	0.36	0.00	0.03
Transition Year	0.05	1.05	1.83
Cooling Time	0.19	0.00	0.00

the most influential input parameters for each output parameter. The Sobol indices are only comparable for each output variable (within each column). The fleet share has the largest impact on final HLW value, while the transition start year has the largest impact on final depleted uranium value and the total idle capacity value in the simulation. Transition start year and cooling time have some influence on the final value of HLW. Fleet share and cooling time do not influence the final depleted uranium value.

Conducting one-at-a-time sensitivity analysis and synergistic analysis on all the input parameters is computationally expensive and produces an overwhelming amount of results. Therefore, using the global sensitivity analysis results, we determine which input variables are the most influential to each performance metric, limiting the number of one-at-a-time and synergistic sensitivity analysis that must be conducted. From Table 5.20, we can inform the types of synergistic and one-at-a-time sensitivity analysis that should be done to understand the transition scenario system better. In Table 5.20, fleet share ratio and cooling time have significant sobol indices on final HLW, therefore, a synergistic sensitivity analysis of fleet share and cooling time is required. In Table 5.20, transition year has a significant sobol index on final depleted uranium, therefore, a one-at-a-time sensitivity analysis of transition year is sufficient to determine the global impact on final depleted uranium. In Table 5.20, transition year has a significant sobol index on total idle capacity, therefore, a one-at-a-time sensitivity analysis of transition year is sufficient to determine the global impact on total idle capacity.

## 5.6 Chapter Summary

### 5.6.1 DYMOND Limitations

For a transition scenario simulation in DYMOND, the user must manually edit the yearly fuel management strategy to define which reactor the recycled part of each fuel type comes from. Having the wrong fuel management strategy results in idle reactor capacity due to the lack of fuel. Therefore, the user has to use trial and error to find a fuel management strategy to minimize or eliminate idle reactor capacity. With a 300-year simulation taking a few hours to run, it quickly becomes tedious and time-consuming.

Idle reactor capacity occurs in the DYMOND simulations during sensitivity analysis because the fuel management strategy is optimized manually for specific scenario parameters. An automatic deployment method (similar to `d3ploy`) should be introduced to determine where the recycled part of each fuel comes from to minimize idle capacity in the simulation. If it existed, it will ease the setting up of transition scenarios, and enables more effective and accurate sensitivity analysis studies.

### 5.6.2 Importance of Different Types of Sensitivity Analysis

The one-at-a-time, synergistic, and global sensitivity analysis methods are all key to analyzing nuclear fuel cycle transition scenarios. In this chapter, we demonstrated each sensitivity analysis type. Each method has advantages. When conducting a comprehensive sensitivity analysis of a specific transition scenario, global sensitivity analysis should be done first to determine which input variables are key to influencing the output variables of interest. One-at-a-time and synergistic sensitivity analysis can then be used together to determine the trends and quantitative impacts of key input variables on performance metrics they most influence. Synergistic sensitivity analysis is used for analyzing the impact of tightly coupled input variables on the performance metrics.

# Chapter 6

## Conclusion

### 6.1 Contributions

The present nuclear fuel cycle in the United States is a once-through fuel cycle of LWRs with no used fuel reprocessing. This nuclear fuel cycle faces cost, safety, proliferation, and spent nuclear fuel challenges that hinder large-scale nuclear power deployment. The U.S Department of Energy identified future nuclear fuel cycles, involving continuous recycling of co-extracted U/Pu or U/TRU in fast and thermal spectrum reactors, that may overcome these challenges. These transition scenarios have been modeled previously in the following nuclear fuel cycle simulators [14, 4]: ORION, DYMOND, VISION, MARKAL, and CYCLUS. However, for many nuclear fuel cycle simulators, the user is required to define a deployment scheme for all supporting facilities to avoid any supply chain gaps or resulting idle reactor capacity. Manually determining a deployment scheme for a once-through fuel cycle is straightforward; however, for complex fuel cycle scenarios, it is not. This thesis developed the capability, `d3ploy`, in CYCLUS that automatically deploys fuel cycle facilities to meet user-defined power demand. This thesis demonstrated `d3ploy`'s set up of the transition from the current LWR fleet to a closed fuel cycle in which transuranics are recycled to fuel MOX LWRs and SFRs. When `d3ploy` used the FFT prediction method and a 2000MW power buffer size, it successfully deployed reactors and supporting fuel cycle facilities to meet a linearly increasing power demand with minimal power undersupply.

Historically, transition scenarios were modeled using a single model in which the transition scenario future is modeled based on assumptions made about various input parameters such as facility size, length of used fuel cooling time, etc. In reality, the transition process inevitably diverges from the modeled scenario. This thesis coupled nuclear fuel cycle simulators, CYCLUS and DYMOND, with Dakota, a sensitivity analysis tool. This work demonstrated one-at-a-time, synergistic, and

global sensitivity analysis with CYCLUS-Dakota and DYMOND-Dakota, to understand the interdependence of input parameters on the transition from the current LWR fleet to a closed fuel cycle in which transuranics are recycled to fuel MOX LWRs and SFRs. The global sensitivity analysis concluded that the transition year input parameter was the most influential to the final depleted uranium and total idle reactor capacity performance metrics, and the fleet share ratio and cooling time input parameters were the most influential to the final high level waste amount in the simulation. The one-at-a-time sensitivity analysis showed that varying transition year from 80 to 84 years increased the final depleted uranium amount by 1.13% and reduced the total idle reactor capacity by 10.36%. The one-at-a-time sensitivity analysis also showed that varying fleet share ratio (MOX LWR:SFR) from 0:100 to 20:80 reduced the final HLW amount by 2%, and varying the used fuel cooling time from 0 to 8 years reduced the final HLW amount by 4%. Therefore, an optimized transition scenario that minimizes final HLW amount, final depleted uranium amount, and total idle capacity must have a fleet share ratio (MOX LWR:SFR) of 20:80, used fuel cooling time of 8 years, and a transition year at 83 years.

This thesis compared CYCLUS-Dakota's and DYMOND-Dakota's sensitivity analysis capabilities and concluded that automated deployment of supporting fuel cycle facilities is crucial for conducting transition scenario sensitivity analyses, to ensure that the simulation adapts to the new parameters by minimizing idle reactor capacity. This work demonstrated that the most influential input variables on each performance metric could be determined through global sensitivity analysis, narrowing-down the one-at-a-time and synergistic sensitivity analyses that need to be conducted. If not, the analyses might include more than 20 input parameters' one-at-a-time and synergistic sensitivity analyses, resulting in difficulties concisely merging them to optimize your transition scenario parameters.

## 6.2 Suggested Future Work

Using the tools developed and demonstrated in this thesis, a comprehensive sensitivity analysis of the EG01-EG30 transition scenario or any scenario of interest can be conducted. The comprehensive sensitivity analysis should begin with a global sensitivity analysis to determine the influential input parameters on all the performance metrics. Following that, one-at-a-time and synergistic

sensitivity analysis can be used to do further analysis of the influential and interdependent input parameters, respectively. Thus, the trends and quantitative impacts of influential input variables on the performance metrics can be determined.

# References

- [1] The Effects of the Uncertainty of Input Parameters on Nuclear Fuel Cycle Scenario Studies. Technical Report NEA/NSC/R(2016)4, OECD, Nuclear Energy Agency, Mar. 2017.
- [2] *Climate Change and Nuclear Power 2018*. Non-serial Publications. INTERNATIONAL ATOMIC ENERGY AGENCY, Vienna, 2018.
- [3] arfc/d3ploy: A collection of Cyclus manager archetypes for demand driven deployment, Sept. 2019. doi:<https://doi.org/10.5281/zenodo.3464123>.
- [4] J. W. Bae, J. L. Peterson-Droogh, and K. D. Huff. Standardized verification of the Cyclus fuel cycle simulator. *Annals of Nuclear Energy*, 128:288–291, June 2019.
- [5] M. Bell. ORIGEN - The ORNL Isotope Generation and Depletion Code. Technical Report ORNL-4628, Oak Ridge National Laboratory, May 1973. Software, Codes & Tools.
- [6] R. W. Carlsen, M. Gidden, K. Huff, A. C. Opotowsky, O. Rakhimov, A. M. Scopatz, and P. Wilson. Cycamore v1.0.0. *Figshare*, June 2014. [http://figshare.com/articles/Cycamore\\_v1\\_0\\_0/1041829](http://figshare.com/articles/Cycamore_v1_0_0/1041829).
- [7] G. Chee. gwenchee/ddwrapper : Gwen's MS Thesis Release, 2019. doi:<https://doi.org/10.5281/zenodo.3530905>.
- [8] G. Chee, J. W. Bae, K. D. Huff, R. R. Flanagan, and R. Fairhurst. Demonstration of Demand-Driven Deployment Capabilities in Cyclus. In *Proceedings of Global/Top Fuel 2019*, Seattle, WA, United States, Sept. 2019. American Nuclear Society.
- [9] G. Chee and K. Huff. arfc/transition-scenarios : MS Thesis Release, Dec. 2019. doi:<https://doi.org/10.5281/zenodo.3569721>.
- [10] G. Chee, G. Westphal, and K. Huff. arfc/dcwrapper : Gwen's MS Thesis Release, 2019. doi:<https://doi.org/10.5281/zenodo.3530964>.
- [11] C. Coquelet-Pascal, M. Tiphine, G. Krivtchik, D. Freynet, C. Cany, R. Eschbach, and C. Chabert. COSI6: A Tool for Nuclear Transition Scenario Studies and Application to SFR Deployment Scenarios with Minor Actinide Transmutation. *Nuclear Technology*, 192(2):91–110, Nov. 2015.
- [12] M. S. Eldred, K. R. Dalbey, W. J. Bohnhoff, B. M. Adams, L. P. Swiler, P. D. Hough, D. M. Gay, J. P. Eddy, and K. H. Haskell. DAKOTA : a multilevel parallel object-oriented framework for design optimization, parameter estimation, uncertainty quantification, and sensitivity analysis. Version 5.0, user's manual. Technical Report SAND2010-2183, 991842, May 2010.

- [13] R. F. Engle. Autoregressive conditional heteroscedasticity with estimates of the variance of United Kingdom inflation. *Econometrica: Journal of the Econometric Society*, pages 987–1007, 1982.
- [14] B. Feng, B. Dixon, E. Sunny, A. Cuadra, J. Jacobson, N. R. Brown, J. Powers, A. Worrall, S. Passerini, and R. Gregg. Standardized verification of fuel cycle modeling. *Annals of Nuclear Energy*, 94:300–312, Aug. 2016.
- [15] L. G. Fishbone and H. Abilock. Markal, a linear-programming model for energy systems analysis: Technical description of the bnl version. *International Journal of Energy Research*, 5(4):353–375, Jan. 1981.
- [16] R. R. Flanagan, J. W. Bae, K. D. Huff, G. J. Chee, and R. Fairhurst. Methods for Automated Fuel Cycle Facility Deployment. In *Proceedings of Global/Top Fuel 2019*, Seattle, WA, United States, Sept. 2019. American Nuclear Society.
- [17] R. Gregg and C. Grove. Analysis of the UK Nuclear Fission Roadmap using the ORION fuel cycle modelling code. In *Proc of the IChemE nuclear fuel cycle conference, Manchester, United Kingdom*, Manchester, United Kingdom, 2012.
- [18] L. Guerin, B. Feng, P. Hejzlar, B. Forget, M. S. Kazimi, L. Van Den Durpel, A. Yacout, T. Taiwo, B. W. Dixon, G. Matthern, L. Boucher, M. Delpech, R. Girieud, and M. Meyer. A Benchmark Study of Computer Codes for System Analysis of the Nuclear Fuel Cycle. Technical Report, Massachusetts Institute of Technology. Center for Advanced Nuclear Energy Systems. Nuclear Fuel Cycle Program, Apr. 2009. Electric Power Research Institute.
- [19] L. Guerin and M. Kazimi. Impact of Alternative Nuclear Fuel Cycle Options on Infrastructure and Fuel Requirements, Actinide and Waste Inventories, and Economics. Technical Report MIT-NFC-TR-111, Massachusetts Institute of Technology, Cambridge, MA, United States, Sept. 2009.
- [20] M. Hammond and A. Robinson. *Python Programming on Win32: Help for Windows Programmers.* ” O'Reilly Media, Inc.”, 2000.
- [21] T. Homma and A. Saltelli. Importance measures in global sensitivity analysis of nonlinear models. *Reliability Engineering & System Safety*, 52(1):1–17, 1996.
- [22] K. D. Huff, J. W. Bae, K. A. Mumma, R. R. Flanagan, and A. M. Scopatz. Current Status of Predictive Transition Capability in Fuel Cycle Simulation. In *Proceedings of Global 2017*, page 11, Seoul, South Korea, Sept. 2017. American Nuclear Society.
- [23] K. D. Huff, M. J. Gidden, R. W. Carlsen, R. R. Flanagan, M. B. McGarry, A. C. Opotowsky, E. A. Schneider, A. M. Scopatz, and P. P. H. Wilson. Fundamental concepts in the Cyclus nuclear fuel cycle simulation framework. *Advances in Engineering Software*, 94:46–59, Apr. 2016. arXiv: 1509.03604.
- [24] R. J. Hyndman and G. Athanasopoulos. *Forecasting: principles and practice*. OTexts, 2018.
- [25] IAEA. Nuclear Fuel Cycle Simulation System (VISTA). Technical Document IAEA-TECDOC-1535, IAEA, Feb. 2007. IAEA-TECDOC-1535, ISBN:92-0-115806-8.

- [26] S. IM. Sensitivity estimates for nonlinear mathematical models. *Math. Model. Comput. Exp.*, 1(4):407–414, 1993.
- [27] S. A. S. Institute. *SAS user's guide: statistics*, volume 2. Sas Inst, 1985.
- [28] J. Jacobson, A. M. Yacout, G. Matthern, S. Piet, D. E. Shropshire, and C. Laws. VISION: Verifiable fuel cycle simulation model. *TRANSACTIONS-AMERICAN NUCLEAR SOCIETY*, 95:157, 2006.
- [29] E. Jones, T. Oliphant, and P. Peterson. *SciPy: Open source scientific tools for Python*, 2001. 2016.
- [30] K. A. McCarthy, B. Dixon, Y.-J. Choi, L. Boucher, K. Ono, F. Alvarez-Velarde, E. M. Gonzalez, and B. Hyland. Benchmark Study on Nuclear Fuel Cycle Transition Scenarios Analysis Codes. Technical report, Tech. Rep. NEA/NSC/WPFC/DOC, 2012.
- [31] M. D. McKay, R. J. Beckman, and W. J. Conover. A comparison of three methods for selecting values of input variables in the analysis of output from a computer code. *Technometrics*, 42(1):55–61, 2000.
- [32] W. McKinney. pandas: a foundational Python library for data analysis and statistics. *Python for High Performance and Scientific Computing*, 14, 2011.
- [33] B. Mouginot, J. B. Clavel, and N. Thiolliere. CLASS, a new tool for nuclear scenarios: Description & First Application. *World Academy of Science, Engineering and Technology, International Journal of Mathematical, Computational, Physical, Electrical and Computer Engineering*, 6(3):232–235, 2012.
- [34] OECD Nuclear Energy Agency. WPFC Expert Group on Advanced Fuel Cycle Scenarios (WPFC/AFCS).
- [35] T. E. Oliphant. *A guide to NumPy*, volume 1. Trelgol Publishing USA, 2006.
- [36] S. Passerini, M. S. Kazimi, and E. Shwageraus. A Systematic Approach to Nuclear Fuel Cycle Analysis and Optimization. *Nuclear Science and Engineering*, 178(2):186–201, Oct. 2014.
- [37] G. Petris and R. An. An R package for dynamic linear models. *Journal of Statistical Software*, 36(12):1–16, 2010.
- [38] D. Petti, P. J. Buongiorno, M. Corradini, and J. Parsons. The future of nuclear energy in a carbon-constrained world. *Massachusetts Institute of Technology Energy Initiative (MITEI)*, 2018.
- [39] K. R. Rao, D. N. Kim, and J. J. Hwang. *Fast Fourier transform-algorithms and applications*. Springer Science & Business Media, 2011.
- [40] Ronacher. Welcome to Jinja2 - Jinja2 Documentation (2.10), 2018.
- [41] E. A. Schneider, C. G. Bathke, and M. R. James. NFCSim: A Dynamic Fuel Burnup and Fuel Cycle Simulation Tool. *Nuclear Technology*, 151(1):35–50, July 2005.
- [42] A. M. Scopatz, A. C. Opotowsky, and P. P. Wilson. Cymetric - A Fuel Cycle Metrics Tool for Cyclus. In *Transactions of the American Nuclear Society*, volume 112 of *Fuel Cycle Simulators*, pages 81–84, San Antonio, TX, June 2015. American Nuclear Society.

- [43] S. Seabold and J. Perktold. Statsmodels: Econometric and statistical modeling with python. In *Proceedings of the 9th Python in Science Conference*, volume 57, page 61. Scipy, 2010.
- [44] N. Sematech. Engineering statistics handbook. *NIST SEMATECH*, 2006.
- [45] A. V. Skarbela, I. M. Rodriguez, F. Alvarez Velarde, A. Hernandez-Sols, and G. Van den Eynde. Quantification of the differences introduced by nuclear fuel cycle simulators in advanced scenario studies. *Annals of Nuclear Energy*, 137:107160, 2020.
- [46] T. G. Smith. *pmdarima: Arima estimators for python*. 2017.
- [47] I. M. Sobol. Global sensitivity indices for nonlinear mathematical models and their Monte Carlo estimates. *Mathematics and Computers in Simulation*, 55(1):271–280, Feb. 2001.
- [48] N. Thiollire, J.-B. Clavel, F. Courtin, X. Doligez, M. Ernoult, Z. Issoufou, G. Krivtchik, B. Leniau, B. Mouginot, A. Bidaud, S. David, V. Lebrin, C. Perigois, Y. Richet, and A. Somaini. A methodology for performing sensitivity analysis in dynamic fuel cycle simulation studies applied to a PWR fleet simulated with the CLASS tool. *EPJ Nuclear Sciences & Technologies*, 4:13, 2018.
- [49] V. Tsibulskiy, S. Subbotin, M. Khoroshev, and F. Depisch. DESAE (Dynamic Energy System-Atomic Energy): Integrated Computer Model for Performing Global Analysis in INPRO Assessment Studies. In *14th International Conference on Nuclear Engineering*, pages 749–753. American Society of Mechanical Engineers, 2006.
- [50] J. A. Turner. Virtual Environment for Reactor Applications (VERA): Snapshot 3. page 81.
- [51] R. Wigeland, T. Taiwo, H. Ludewig, M. Todosow, and W. Halsey. Nuclear Fuel Cycle Evaluation and Screening Final Report. Technical Report INL/EXT-14-31465, U.S. Department of Energy, 2014.
- [52] A. M. Yacout, J. J. Jacobson, G. E. Matthern, S. J. Piet, and A. Moisseytsev. Modeling the Nuclear Fuel Cycle. In *The 23rd International Conference of the System Dynamics Society,” Boston*. Citeseer, 2005.
- [53] G. Zhang, T. Sumner, and T. Fanning. Uncertainty Quantification of EBR-II Loss of Heat Sink Simulations with SAS4a/SASSYS-1 and DAKOTA. page 14.
- [54] X.-Y. Zhang, M. Trame, L. Lesko, and S. Schmidt. Sobol Sensitivity Analysis: A Tool to Guide the Development and Evaluation of Systems Pharmacology Models: Sensitivity Analysis of Systems Pharmacology Model. *CPT: Pharmacometrics & Systems Pharmacology*, 4(2):69–79, Feb. 2015.
- [55] F. Alvarez Velarde, P. Len, and E. Gonzalez-Romero. EVOLCODE2, a combined neutronics and burn-up evolution simulation code. *Actinide and Fission Product Partitioning and Transmutation*, page 443, 2007.